

# **Appendix A-1: Engineering**

# East Hagatna, Guam CAP Section 14 Emergency Shoreline Protection

Draft Integrated Feasibility Report and Environmental Assessment

August 2025

# **Table of Contents**

1. Gener	ral	3
1.1. P	revious Reports	3
1.2. P	roblem Description	4
2. Existi	ng Site Conditions	4
2.1 Stud	ly Area	4
2.2. C	limatology	7
2.3. T	ropical and Extratropical Storms	7
2.4. E	l Niño Southern Oscillation Cycles	8
2.5. W	/inds	9
2.6. T	sunamis and Earthquakes	.10
2.7. B	athymetry and Topography	.11
2.8. W	/ater Levels	.12
2.8.1.	Tides	.13
2.8.2.	Sea Level Change	.13
2.8.3.	Extreme Water Levels	.15
2.9. W	/aves	.16
2.9.1.	Typical Conditions	.16
2.9.2.	Extreme Wave Frequency Analysis	.17
2.10.	Design Waves & Water Levels	.20
3. Nume	rical Modeling	.23
3.1. STV	VAVE	.23
3.2. M	lodel Domain	.23
3.3. Offs	shore Boundary Spectra	.24
3.4. M	lodel Execution	.25
3.5. M	lodel Outputs	.25
4. Engin	eering Alternatives	.29
4.1. P	reliminary Array of Measures	.29
4.2. N	o Action	.29
4.3. R	evetment	.30
4.4. V	ertical Seawall Measures	.38
4.5. P	recast Concrete Wall (Tentatively Selected Plan)	.39
4.6. C	oncrete Rubble Masonry Wall	.41
4.7. Sec	cant Wall (Screened Out)	.43
4.8. P	ermeation Grouting (Screened Out)	.45
4.9. B	each Nourishment (Screened Out)	.46

5	. References	.47
6	. Model Output Appendix	.48
7.	. Summary	.46

#### 1. General

The following describes the technical assessment completed as part of the U.S. Army Corps of Engineers (USACE) Continuing Authorities Program Section 14 East Hagåtña Emergency Shoreline Protection Study in Hagåtña, Guam. The purpose of the study is to conduct a feasibility level evaluation of the existing coastal/hydraulic conditions including extreme water levels, wave climate evaluation, and sea level change that affect the study area, and evaluation of the proposed shoreline stabilization alternatives to determine the recommended plan.

# 1.1. Previous Reports

Previous Federal reports, listed below, have assessed various conditions within the region and are referenced within this document as needed.

- Draft East Agana, Territory of Guam, Detailed Project Report and Environmental Assessment, U.S. Army Corps of Engineers, Honolulu Engineer District, July 1993 (terminated at Sponsor's request). The report identified a federal interest in shore protection measures along two reaches of the East Agana shoreline. The benefit- to-cost ratio for five alternatives evaluated ranged from 1.7 to 1.9.
- East Agana, Territory Guam, Shore Protection Study, Reconnaissance Report, U.S. Army Corps of Engineers, Honolulu Engineer District, April 1990. The reconnaissance level report is the predecessor to this feasibility phase investigation. It identified the coastal flooding problem in East Agana and identified a potential solution to the problem.
- Agana Bayfront Storm Surge Protection Study, Territory of Guam (Draft Feasibility Report and Environmental Impact Statement), U.S. Army Corps of Engineers, Honolulu Engineer District, December 1988. This feasibility level report identified the coastal flooding problems and needs of the low-lying areas of Agana Bay. Various measures available to reduce coastal flood damages caused by storm surge and their environmental consequences were investigated.
- Typhoon Stage-Frequency Analysis for Agana Bay, Guam (Draft Technical Report),
  U.S. Army Corps of Engineers, Coastal Engineering Research Center, Waterways
  Experiment Station, July 1987. The purpose of the study was to determine the frequency
  of flood levels along the shoreline of Agana Bay that are caused by the combined effects
  of astronomical tides and typhoon-induced water levels. The results of this study have
  been incorporated into the analyses contained in this report.
- Guam Comprehensive Study Agana Bay Typhoon and Storm-Surge Protection Study (Technical Documentation), U.S. Army Corps of Engineers, Pacific Ocean Division, January 1984. This was the first report to attempt identification of the problems and needs for coastal flooding in the Agana Bay area. Due to the lack of data, the documentation did not include typhoon stage- frequency analyses.
- Flood Insurance Study, Territory of Guam, U.S. Army Corps of Engineers, Pacific Ocean Division, September 1983. The study was completed by the U.S. Corps of Engineers for the Federal Emergency Management Agency (FEMA) under the authorities of the National Flood Insurance Act of 1968 and the Flood Disaster Protection Act of 1973. The flood insurance study investigated the existence and severity of flood

hazards on the island of Guam. The study also developed flood risk data for various areas of the community that have been used to establish actuarial flood insurance rates and assist the community in their efforts to promote sound flood plain management. A section of the report covered the problems of coastal flooding and documented several accounts of damages by wind generated waves.

- Shoreline Investigations, Agana, Guam, U.S. Army Corps of Engineers, Honolulu Engineer District, September 1981. This report described existing shoreline features, structures, and conditions and showed the boundaries of storm surge and storm wave flooding at Agana Bay.
- Guam Comprehensive Study Stage 1 Report, U.S. Army Corps of Engineers,
  Honolulu Engineer District, August 1979. The reconnaissance level (Stage 1) report
  identified the water resource problems and needs for the Territory of Guam. The Guam
  Comprehensive Study was the parent study for the Agana Bayfront feasibility study. The
  Stage 1 report included problem identification, planning objectives, potential
  management and nonstructural measures, and potentially significant impact for regional
  harbors, water supply, flood plain management, and shore protection and beach
  restoration.

# 1.2. Problem Description

The low-lying coastline of East Hagåtña is subject to infrequent but severe storm wave attack. The much higher than usual wave heights reaching the shoreline during severe storm events in combination with a limited sediment supply, have caused erosion to the beach and resulted in undermining of the existing seawall. This continuous damage to the existing shore protection structure has put Marine Corps Drive and public utilities in the immediate vicinity of the project area at imminent risk. Future sea level rise will continue to exacerbate this condition and cause erosion and the resulting damage to accelerate. Due to the observed ongoing shoreline erosion along Marine Corps Drive, replacement shore protection alternatives will be explored within this feasibility study.

# 2. Existing Site Conditions

The following is a general description of the existing conditions of the project area, as known at the time of this study, which are utilized in developing the proposed alternatives for the site.

#### 2.1 Study Area

The Mariana Islands are a north-south archipelago arc chain consisting of 15 relatively small islands with the total landmass of approximately 400 square miles of which 215 square miles comprise the island of Guam. Guam is the largest and southernmost island of the Mariana Islands. Located 3,950 miles west of Hawaii, Guam is the westernmost point of the United States. The island is approximately 30 miles long, 4 to 12 miles wide, with 110 miles of shoreline. Hagåtña Bay is centrally located on the west coast of the island of Guam. The project area is within Hagåtña Bay between the villages of Asan and Tamuning and spans approximately 1630 ft long (Figure 1), this length is reduced from the 2100 ft of existing seawall located in the area in order to more concisely focus on the areas of greatest erosion concern. These areas were identified during site visits (Figures 2-5).

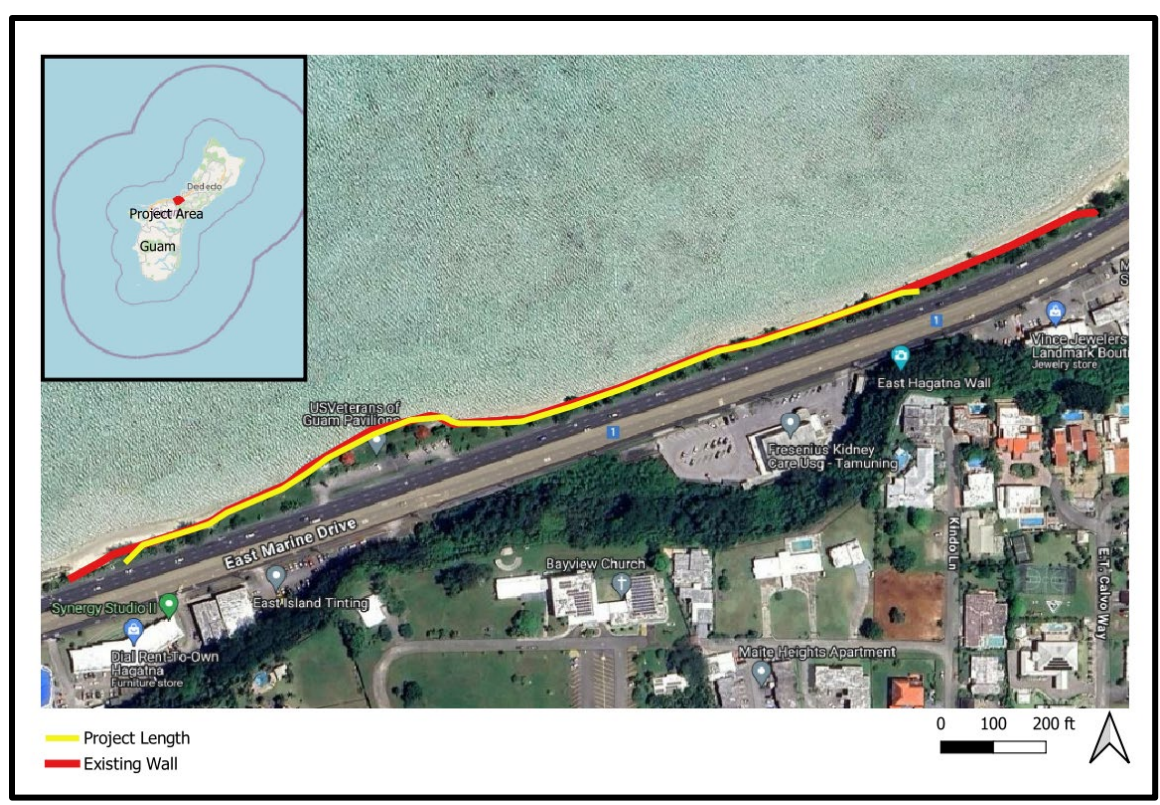


Figure 1. Project Area Map

The project area is fronted by an extensive fringing reef. The reef is approximately 0.5 miles wide, with maximum water depths of less than 6 feet. The reef is continuous for most of its length within Hagåtña Bay, and is highly effective at dissipating most wave energy from reaching the beach during periods of typical water levels and wave heights. Due to the curved shape of the bay and rocky headlands on either end, the shoreline within this area is also sheltered from the prevailing wind and wave energy from the northeast to southwest. Just to the west of the project area is Agana Small Boat Harbor, a federally authorized and maintained harbor. Also located near the center of the project area is the US Veterans of Guam Pavilions Park. The park protrudes oceanward from the coastline. The beach within the project area is narrow, ranging from approximately 0 ft to 50 ft wide, with a mean width of 20 ft wide. The beach does not appear stable and shows evidence of past erosion, particularly around the public park. This erosion is thought to be caused by a combination of chronic erosion with storm induced elevated water levels and wave energy.

An existing seawall runs the length of the project area. This wall's foundation was built approximately at or below the shoreline elevation at the time of construction (1990's) and was not placed on hard substrate or constructed footings. Since construction, erosion of the sandy shoreline underneath the wall has resulted in many sections being critically undermined, thus degrading the overall stability and functionality of the wall.

Loss of foundation material has caused sinkholes to form in the area landward of the wall, which have often been filled with grout to avoid a continual safety hazard. Due to the continued exposure of the beach to elevated water levels and wave energy, this structure will continue to be susceptible to further undermining and eventual failure.

Figure 2 to Figure 5 represent a sample of the general conditions of the existing seawall.



Figure 2. Sinkhole along landward side of wall in backfill



Figure 3. Eastern section of the wall undermined due to erosion



Figure 4. Undermining of the structure around the park pavilion



Figure 5. Voids where wall was constructed around trees that have since been removed or fallen

The shoreline was assumed to be relatively consistent throughout the project limits with subtle changes to the orientation, profile and elevation of the foreshore and beach elements. There is some variation along the backshore area throughout the project limits, with varying widths of backfill between the shoreline and Marine Corps Drive Road. As mentioned, the sandy foreshore varies from 0 to 50 feet wide along the project area.

Sparsely grouped trees lie along the project area, with 2-3 trees being integrated into the existing structure. At the public park there are two sets of access stairs which lead to the water. Due to the critical undermining of the area, there is some sinking of the adjacent backfill near the stairs, as well as cracks in the structure.

There are 3 culverts along the project length, all of which have significant debris clogging their outlets. It is assumed that these culverts are strictly for storm water management; no permanent inland waterway lies within the project limits.

# 2.2. Climatology

The Guam climate is tropical, with warm and humid conditions throughout the year. The surrounding ocean has a year-round temperature of 81 degrees and is largely responsible for the island's climate. There are two distinct seasons, defined by variations in wind and rainfall. A dry season extends from January through May, and a wet season from July through November. December and June are transitional months. Annual rainfall averages are typically above 80 inches. Easterly trade winds occur throughout the year but are dominant during the dry season. From July to October the winds become variable, and the occurrence of typhoons increases.

## 2.3. Tropical and Extratropical Storms

In the western Pacific Ocean, west of the International Date Line, hurricanes are referred to as typhoons. This term is analogous to hurricanes in the eastern Pacific Ocean or western Atlantic Ocean. The low latitude location of Guam is favorable for tropical storm and typhoon formation and passage. The island often experiences typhoon impacts which are highly dependent on the storm track. Typical typhoon impacts include wind and rainfall damage to buildings, roads and crops, and coastal inundation and resulting damage during periods of high waves and water levels.

Typhoons are tropical storms with winds of 65 knots or greater with associated intense rainfall. Although severe typhoons occur in the western Pacific throughout the year, the period from July to December is characterized as the primary typhoon season. From 1900 to 1941 Guam was affected by 23 typhoons, and from 1945 to 1990 Guam was affected by 37 typhoons. Gaps in the data exist from 1942-1944 when Guam was occupied by Japanese forces (Weir 1983). In 1962, Typhoon Karen destroyed 90% of the homes on Guam, with estimated peak sustained wind of 135 knots (Rupp and Lander, 1996). Typhoon Pamela in 1976, with sustained winds of 120 knots, stalled off the west coast of Guam for several days, resulting in extensive damage to coastal facilities. Typhoon Yuri in 1991 caused extensive beach erosion and structural damages with gusts up to 100 knots. The storm also produced extreme waves in the area.

Typhoon Omar and Gay devastated the island in 1992, with sustained winds of 170 knots and 87 knots, respectively. Then in 1997, Typhoon Paka, with an estimated maximum sustained wind speed of 107 knots at Apra Harbor, destroyed roughly 1,500 buildings, leaving an estimated 5,000 people homeless (EQE International 1998 and NCDC 1997). Typhoon Pongsona in 2002, left more than 60% of the island's water wells inoperable and destroyed approximately 1,300 homes (FEMA 2003 and Gillespie 2002). The most recent typhoons to affect Guam was Typhoon Wutip in February 2019, with sustained winds of 130 knots and Typhoon Mawar in June 2023, with sustained winds of 122 knots.

Extratropical storms are generated far from the island of Guam. These types of events can be generated by an extratropical storm in the northern or southern Pacific Ocean or a large event in the Southern Ocean. They are characterized by waves generated far away from the project site that propagate across the open ocean, interact with each other, and finally impact the project site with large waves. Distant typhoons are also capable of generating a wave-only event if the storm is large enough and traveling in specified direction in relation to the island. The difference between a typhoon condition and the extratropical swell condition is the longer period of the swell conditions along with a minimal increase to the nearshore water levels.

# 2.4. El Niño Southern Oscillation Cycles

Climate impacts sea levels, coastal storm surge, and tropical cyclone intensity, and is significantly tied to El Niño Southern Oscillation (ENSO) fluctuations. ENSO consists of three phases, Neutral, El Niño and La Niña, with average durations between 9 and 18 months. The relationship between El Niño and La Niña cycles and the Southern Oscillation is a relationship between oceanic sea surface temperature (SST) and the atmospheric pressure gradient, respectively. In neutral conditions, the Pacific trade winds are driven westward owing to changes in the atmospheric pressure gradient across the Pacific, where lower atmospheric pressures in the western Pacific and higher pressure to the east drive trade winds and warmer SST westward. Consequently, cooler SSTs are observed in the eastern Pacific. Higher SSTs transfer heat to the atmosphere, which, in turn, change the pressure gradient. In other words, the pressure gradient affects the SST and the SST affects the pressure gradient. This circulation is referred to as the Walker Circulation.

Under El Niño conditions, trade winds weaken, allowing warmer western Pacific waters to migrate eastward. This results in lower sea levels and SST in the western Pacific and higher sea levels and SST in the eastern Pacific. Sea surface elevations can fluctuate from El Niño and La Niña events by as much as 0.7 to 1.0 feet (IPRC, 2014). During El Niño the western Pacific experiences reduced rainfall and drought conditions, while the

eastern Pacific experiences wetter conditions. Under La Niña conditions, trade winds increase, resulting in significant pooling of warm water and higher SST in the western Pacific, increased sea levels, and increased convection. Correspondingly, lower SST, lower sea levels, and reduced convection occurs in the eastern Pacific (NOAA, 2021). See Figure 6 below for an illustration of ENSO cycles.

Tropical cyclones thrive off warm ocean waters. El Niño effectively discharges heat into the ocean, leading to intensified tropical cyclones (Rupic et al., 2018). ENSO affects climate and weather patterns which impact precipitation, cyclones, and sea levels. ENSO adds variability to recorded water levels, which affects the total water levels at the project site.

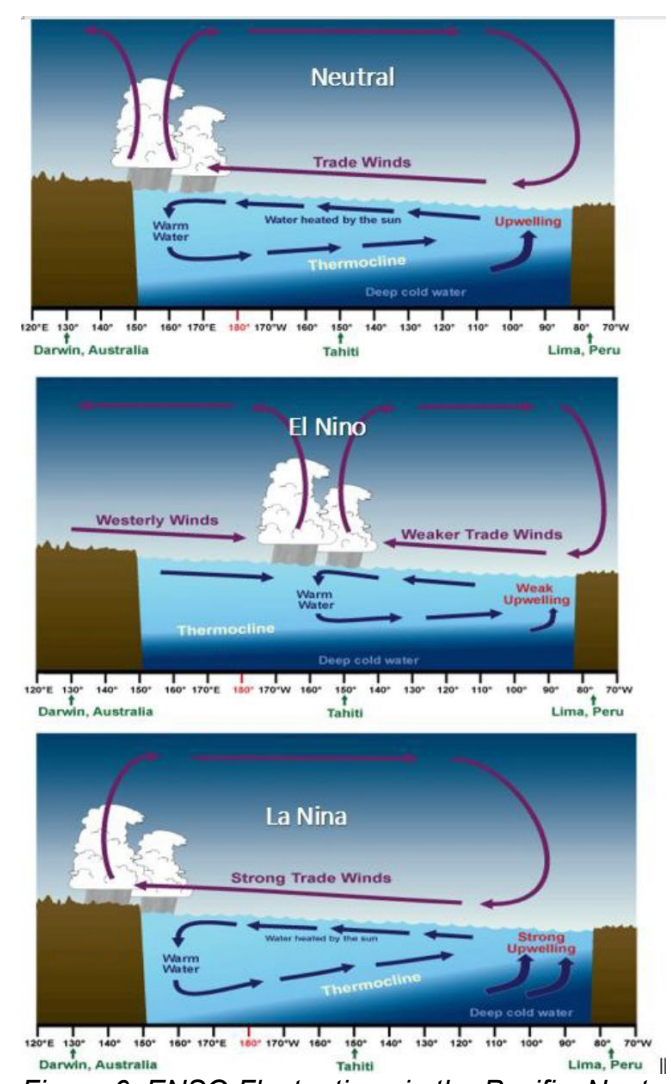


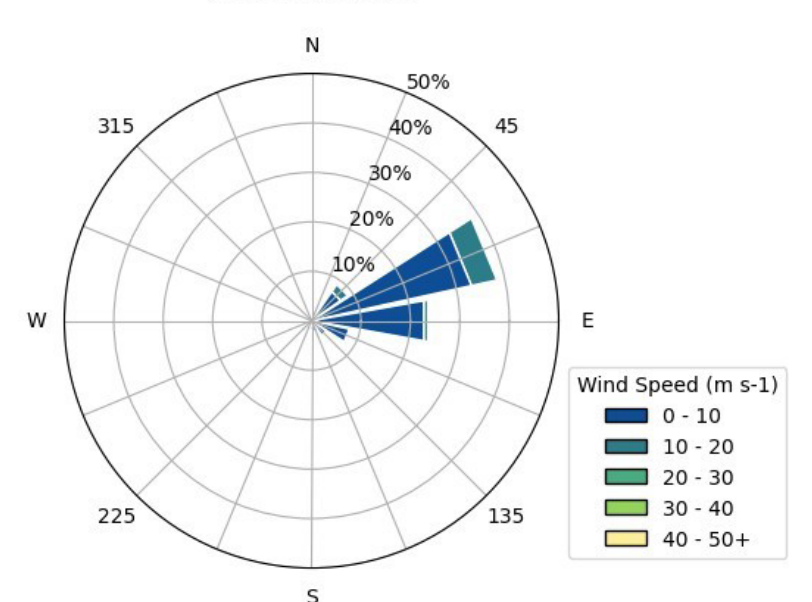
Figure 6. ENSO Fluctuations in the Pacific: Neutral, El Niño, and La Niña (Source: NOAA)

#### 2.5. Winds

The USACE Wave Information Study (WIS) provides offshore wind statistics at selected stations around Guam. The nearest WIS station to the East Hagåtña project area is station 81416, located at 14° N and 144.5° W, approximately 40 miles from the project site. A wind rose

displaying the frequency (%), wind speed (in meters/second), and wind direction (wind coming from) for 1980-2019 is shown in Figure 7. The dominant winds in Guam are the easterly trade winds, which approach from the sector northeast through east-southeast. They occur approximately 70 percent of the time throughout the year, but are particularly pronounced during the dry season, January through April, when they occur more than 90 percent of the time. Typical trade wind speeds fall in the 7 to 16 knot (3.6 to 8.2 m/s) range. Wind speeds greater than 21 knots (10 m/s) only occur about 5 to 10 percent of the time. Wind directions are variable with frequent calms during the main typhoon season from July to December. Trade winds, although they occur less frequently than during the dry season, are still the most common winds during this period. The highest percentage of strong winds come from the northeast.

WIS Pacific Hindcast: 81416 1980-02-01T00:59:44Z - 2020-01-01T00:00:00Z Loc: 144.5°/14.0° Depth: -999.99 [m] Total Obs: 349896



S Figure 7. Wind rose from WIS Station 81416 near Guam

From 1999 to 2020, the average yearly max wind speed recorded at NOAA Station 630000 located in Apra Harbor, was 43.4 knots. The average wind speed was 10.4 knots, with a modal wind speed of 2.6 knots. During this twenty-one-year record there were three incidences of recorded sustained wind speeds with typhoon intensities - in December 1999 (142 mph), November 2000 (169 mph), and December 2001 (142 mph). This indicates that while Guam is affected by one or more typhoons almost every year, they often do not pass directly over Guam, and/or that high winds can be very localized. Data records can also be limited by failure of the measurement equipment during high winds.

#### 2.6. Tsunamis and Earthquakes

An earthquake is a series of seismic waves created by the sudden release of stored energy in the Earth's crust. A tsunami is a long period open ocean wave or series of waves typically caused by an earthquake or underwater landslide. There have been 12 major earthquakes and 4 tsunamis recorded in Guam. The most significant earthquake event occurred in August 1993, with an 8.1 magnitude. No deaths were reported, but approximately 50 people were injured and

more than \$200 million in property damage were reported (Brunsdon, 1993). The 1993 earthquake caused land subsidence, affecting Guam's relative sea level change rates (see Section 2.8.2). This earthquake also generated a minor tsunami. A report from Lander et al. (2002) that considered the risk of destructive tsunamis in Guam, notes that locally generated tsunamis are most likely to affect the less populated east coast due to the location of the Marianas Trench, which is the main origin of Guam's earthquakes. The most recent tsunami event to affect Guam occurred in February 2010. The tsunami was generated from an 8.8 magnitude earthquake near Chile and measured 0.5 ft at Apra Harbor.

# 2.7. Bathymetry and Topography

The recently available 2020 National Ocean and Atmosphere Administration (NOAA) National Geodetic Survey (NGS) topography and bathymetry (topobathy) LiDAR was retrieved from the NOAA digital coast data access viewer ( https://coast.noaa.gov/digitalcoast/tools/dav.html) for evaluation of nearshore and foreshore elevation conditions. The LiDAR data accuracy is set according to the National Map Accuracy Standards (NMAS) which requires vertical accuracy with a root mean square error (RMSE) of ±7 feet and horizontal accuracy within ±40 feet for 90% of tested points for 1:24,000 scale maps. These standards ensure that LiDAR-derived products meet the reliability needed for detailed topographic and mapping applications. All topo lidar data were collected simultaneous to meet United States Geological Survey, Quality Level 1 (USGS QL1) with a minimum of 8 pts per square meter at an accuracy of 10cm RMSEz. A minimum of 2 points per square meter were acquired for bathymetric lidar data. The LiDAR had a resolution of 1-meter meaning that the LiDAR system can distinguish objects or features that are at least 1 meter apart on the ground. This resolution indicates the smallest distance between two separate points that the LiDAR can reliably detect and measure. A 1-meter resolution is considered moderate for LiDAR applications and is suitable for various mapping, terrain modeling, and infrastructure planning tasks where a balance between detail and data volume is necessary. The Topobathy data was also used in the numerical modeling effort discussed below in Section 3.

The Guam Vertical Datum of 2004 (GUVD04) is the official vertical datum for Guam and is approximately equal to Mean Sea Level (MSL). The following describes the data's coordinate system and datums:

Coordinate System: UTM (Universal Transverse Mercator) Zone 55N

Horizontal Datum: NAD83, meters
 Vertical Datum: GUVD04 (~MSL)

The topobathy water depths and elevations range from deep water (158 ft depth) to landward elevation of +148 ft relative to MSL. Figure 8 illustrates the bathymetry and topography contours of the project site and surrounding areas. From the bathymetry data, the depth of a consolidated limestone layer fronting the project area and underlying sandy shoreline was determined to be at 1.6 to 2.6 ft. (-0.5 to -0.7 m) below MSL. Also determined was the approximate elevation of the existing wall at 7.5 to 8.9 ft. (2.3 to 2.7m) above MSL. Based on this information for a typical section of the proposed alternatives, -2.6 ft. MSL will be used as the assumed elevation for the limestone layer, and +8.9 ft. MSL will be assumed as the existing wall's crest elevation. The elevation profiles along the project area are shown in Figure 9.



Figure 8. East Hagåtña Shoreline Bathymetric and Topographic contours in feet

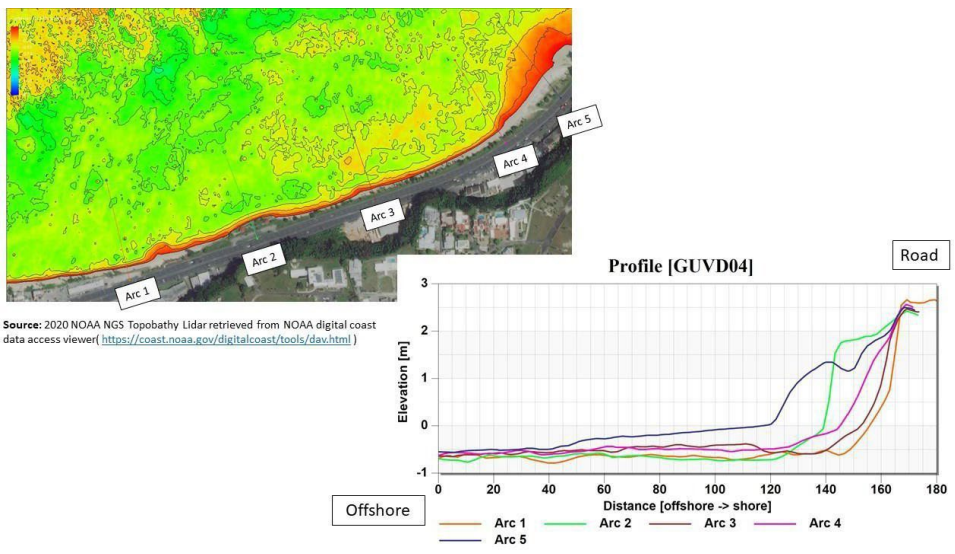


Figure 9. Typical Elevation Profiles along the Project Area

## 2.8. Water Levels

The closest water level station to the study area, maintained by the National Oceanographic and Atmospheric Administration (NOAA), is Apra Harbor, Guam (Station 1630000). The tidal station is located 8.3 miles southwest of the project area, within Apra Harbor. Due to this protected location, the water level station would be expected to capture water level components including astronomic tide, sea level rise, seasonal fluctuations, and some storm surge due to wind setup and reduced central pressure during a tropical cyclone. It is not expected to capture elevation of the water level due to wave setup caused by wave breaking, which is experienced at the project area during both tropical and extratropical events. This introduces a potential source of uncertainty in the use of this station to fully represent extreme water levels.

#### 2.8.1. Tides

Tides in the western Pacific are mixed-type, semi-diurnal with two highs and two lows of different levels every lunar day. Tides in the open ocean typically have spatial characteristics on the order of hundreds of miles. Tidal ranges tend to be small, on the order of 2 feet, and are spatially uniform.

The Apra Harbor, Guam tidal gauge was established in 1948 and has been in continuous operation since 1989. Tidal datums relative to Mean Sea Level (MSL) from this station are summarized in Table 1. The local vertical datum, GUVD04, is 0.01 feet above MSL, and the two datums are used interchangeably throughout this analysis.

Station: 163	Station: 1630000, Apra Harbor, Guam										
<b>Epoch:</b> 1983-2001											
Units: Feet	Reference Datum: N	ISL .									
Datum	Value	Description									
MHHW	0.97	Mean Higher-High Water									
GUVD04	0.01	Guam Vertical Datum of 2004									
MSL	0.00	Mean Sea Level									
MLLW	-1.37	Mean Lower-Low Water									
Max Tide	2.92	Highest Observed Tide									
Max Tide Date & Time	08/28/1992 18:54	Highest Observed Tide Date & Time									
Min Tide	-3.71	Lowest Observed Tide									
Min Tide Date & Time	10/24/1972 00:00	Lowest Observed Tide Date & Time									

Table 1. Tidal Datums at Apra Harbor, Guam

#### 2.8.2. Sea Level Change

The USACE considers potential relative sea level change in every project undertaken within the tidally influenced zone. Engineering Regulation (ER) 1100-2-8162 (Dept. Army, 2019) establishes procedures for projecting sea level change into the future based on global sea level change rates, local historic sea level change rate, base year of project analysis, and the number of years in the period of analysis. It is generally accepted that sea level will continue to rise and that the rate of rise may accelerate due to climatic changes. The USACE provides guidance on the calculation of sea level change and its application to the planning process. This regulation requires that three scenarios be evaluated which result in low, intermediate, and high predictions of sea level rise. The low value is based on an extrapolation of the local historic sea level rise rate. The intermediate and high values are based on the National Research Council (NRC) sea level rise predictive Curves I and III, respectively.

Over the past two decades, sea level trends have increased in the western tropical Pacific Ocean with rates that are approximately three times the global average. Several papers including Merrifield and Maltrud (Merrifield and Maltrude, 2011) have shown that the high rates of SLC recorded are caused by a gradual intensification of Pacific trade winds since the early 1990s. Multi-decadal tradewind shifts cause sea level variations which can lead to linear trend changes over 20 year time scales that are as large as the global SLC rate, and even higher at individual tide gauges, such as Apra Harbor, Guam (Merrifield 2011, Merrifield et al. 2012).

Due to the variability in MSL trends in the western Pacific, and the short post- earthquake trend (1993-present) at Apra Harbor, Guam, the rate of relative SLC in Guam is estimated by using

the global eustatic rate of SLC, +1.7 mm/year, added to a measured rate of Vertical Land Movement (VLM) rate of -0.889 mm/year (as reported by the NASA Jet Propulsion Laboratory website https://sideshow.jpl.nasa.gov/post/series.html – an average of two monitoring stations on Guam). Since eustatic sea level is rising, and the land is subsiding, this results in a relative SLC rate of 2.59 mm/year (= +1.7 mm/year – (-0.89 mm/year)) or 0.0085 feet/year for Guam.

The USACE SLC calculator was used to plot the three potential curves based on this rate, shown in Figure 10. The curves show that by halfway through project planning horizon in 2050, the relative SLC in the area will be be 0.5 feet (low curve), 0.78 ft (intermediate curve), or 1.73 ft (high curve), and by the end of the project planning horizon in 2075, the relative SLC in the area will be 0.7 feet (low curve), 1.3 ft (intermediate curve), or 3.3 ft (high curve) relative to the existing MSL datum (as well as GUVD04). By the end of the adaptation planning horizon in 2125, the relative SLC in the area is projected to be 1.10 ft (low curve), 2.7 ft. (intermediate curve), or 7.6 ft. (high curve). Also shown on the plot is the +8.9 ft MSL elevation of the existing sea wall crest. This threshold is not exceeded by still water elevation over the course of the adaptation planning horizon. The USACE Sea Level Tracker tool was also utilized to compare existing recorded water levels at Apra Harbor with SLC projections. Figure 11 shows the SLC curves, the 5-year moving average in cyan, and the 19-year moving average in dark blue. The moving averages illustrate the significant variability in the SLC rate as described above. Since the 1993 earthquake, the 19-year moving average trend has exceeded the "high" curve due to land subsidence and tradewind intensification. The 5-year moving average suggests that this trend may be reversing in recent years, and is more closely tracking the "intermediate" curve. Sensitivity to the various SLC scenarios was evaluated and will be discussed in later sections.

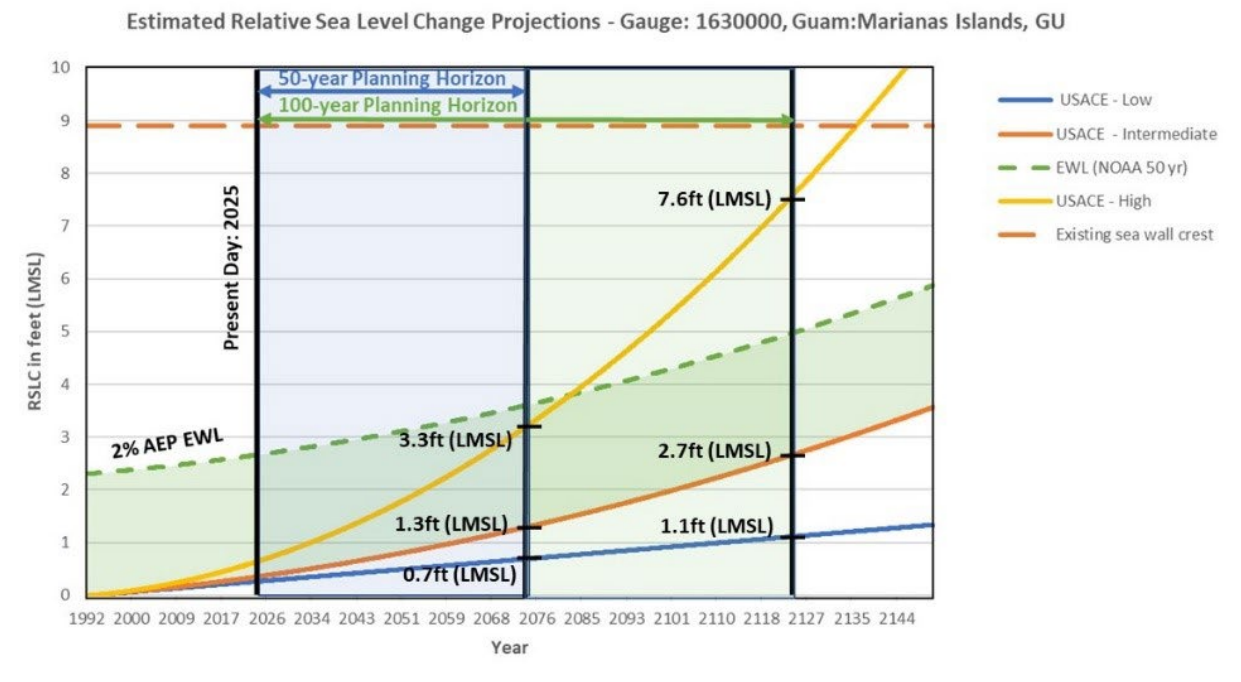


Figure 10. USACE SLC Curves for Guam Including 50-year Planning Horizon and 100-year Adaptation Horizon

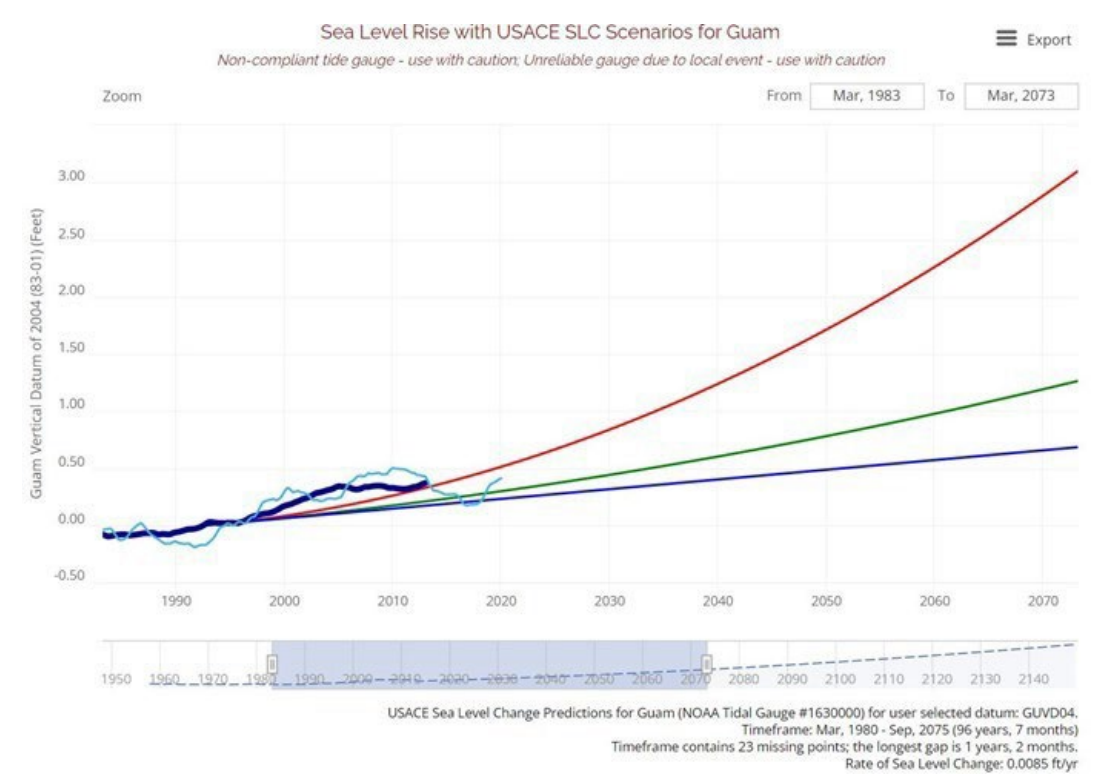


Figure 11. USACE Sea Level Tracker for Guam Including 5-year (cyan) and 19- year (blue) Moving Average

## 2.8.3. Extreme Water Levels

The extreme water level (EWL) is comprised of short-term, storm-driven water level changes superimposed on the astronomical tides. The probabilistic frequency of extreme water levels for the project region are shown in the annual exceedance probability (AEP) curves, determined at the NOAA water level station in Apra Harbor Guam (Figure 12). The annual exceedance probability curves show the extreme water level elevations as a function of return period in years. These elevations are determined after the Mean Sea Level (MSL) trend is removed. As shown, the 2% AEP or 50-year return period water elevation at Apra Harbor Guam is approximately 1.5 ft (0.46 m) relative to MHHW or 2.29 ft (0.71 m) relative to MSL. This additional water level component is superimposed on the intermediate curve shown in Figure 11 to assist with visualization of extreme water level occurrences on top of rising sea level for present day and throughout the project planning horizon.

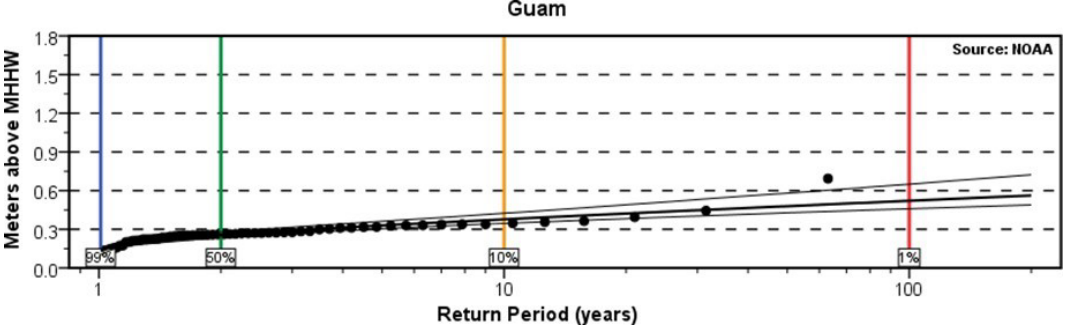


Figure 12. AEP curves relative to MHHW

#### 2.9. Waves

There are three distinct wave patterns near Guam: local wind (trade wind) generated waves, long period swell energy generated by distant storms, and waves associated with tropical cyclones. Trade wind waves are typically from northeast through east- southeast, with wave heights in the range of 1 to 6 feet (0.3 to 2 m) and wave periods between 5 to 10 seconds. Swell waves from distant storms (usually in the north Pacific) can range from 6 to 18 feet (2 to 6 m) in height and have wave periods from 10 to 16 seconds. Tropical storm and typhoon waves can approach from almost any direction (though the storms typically track east to west or southeast to northwest), resulting in waves up to 40+ feet (13+ m) in deep water and wave periods in the 8 to 14 second range. The most common condition is trade wind generated waves, which due to the orientation of Guam's coastline, do not affect the western side of the island. Due to incident wave direction and shoreline orientation within the project area, only swells originating in the west and tropical cyclones have the potential to cause damages to the project area.

# 2.9.1. Typical Conditions

The USACE's Wave Information Study (WIS) is a 39-year (1980–2022) wave hindcast, which can be used to perform wave climate analysis at a given station location. The water depths at the station are greater than 10,000 ft. Basic statistics of information recorded at this virtual point is shown in

Table 2. The largest calculated wave height was generated from a tropical storm (Typhoon Yuri – 1991).

Statistic	Value
Average wave height:	6.1 ft
Standard deviation of wave height:	2.2 ft
Average wave period:	9.6 sec
Standard deviation of wave period:	1.5 sec
Maximum wave height:	49.5 ft
Period associated w/ max wave height:	15.1 sec
Direction associated w/ max wave height:	99.0 deg
Date associated w/ max wave height:	11/27/1991 17:00
Total number of wave records:	280,511

Using WIS Station 81416, the typical wave climate oceanward of the northwestern side of Guam can be determined. Figure 13 shows the location of the WIS station relative to the project area as well as the frequency of occurrence for various wave heights and associated wave directions in the area. As previously discussed, the shoreline orientation within the project area and the presence of the fringing reef significantly reduces the amount of wave energy that reaches the project area.

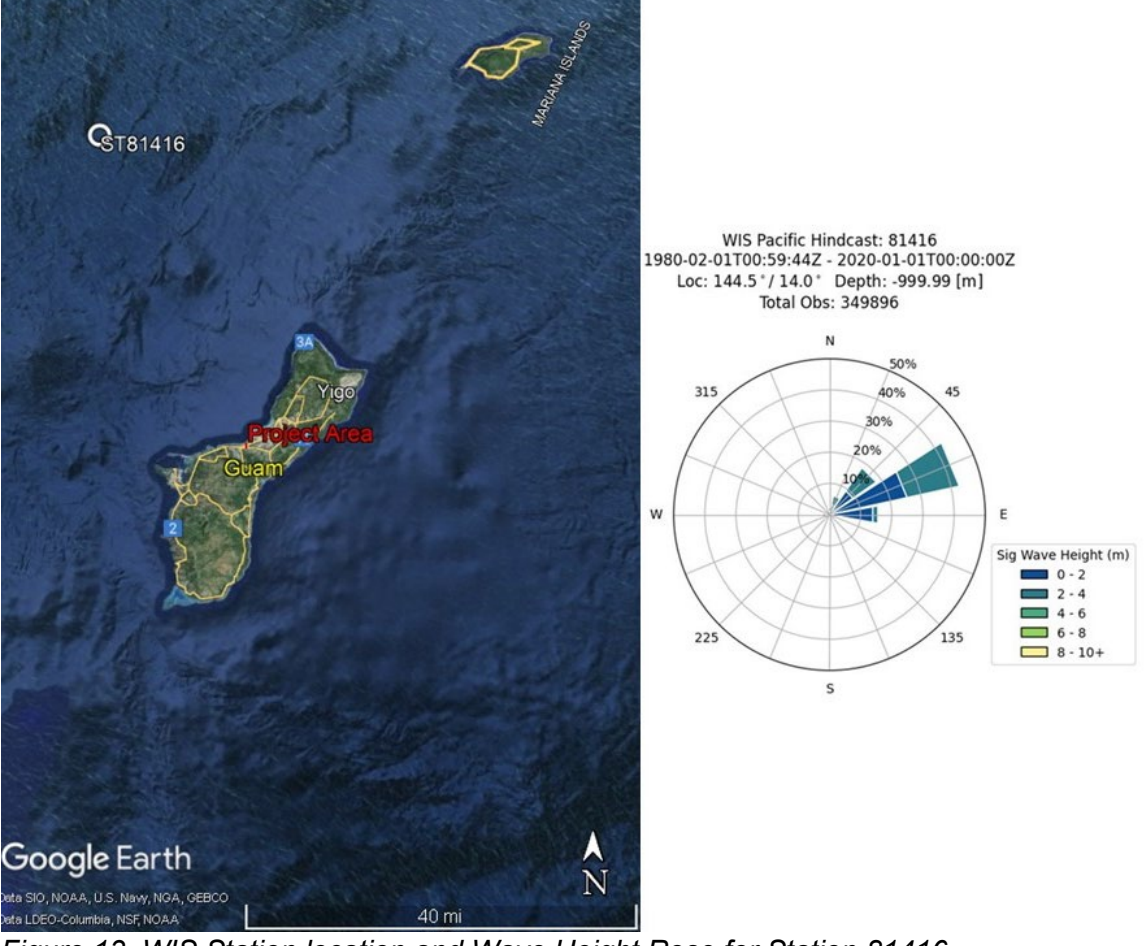


Figure 13. WIS Station location and Wave Height Rose for Station 81416

Only typhoons and swells generated from the west through north are included in this analysis as they have a potential to produce damages to island infrastructure at this location.

#### 2.9.2. Extreme Wave Frequency Analysis

Due to the project area's location on the west central side of Guam, it is assumed that only waves propagating from the west to the north of the island, regardless of the generation source, may impact the project location. To verify this assumption the nearshore steady state wave model, STWAVE, was used to evaluate the directional sensitivity for the project area. STWAVE is discussed in more detail in Section 3. The directional sensitivity analysis, was conducted by propagating 2 wave heights (16.1 ft and 49.5 ft) and 2 peak periods (10 and 15 seconds) in conjunction with 5 mean wave directions (45°, 0°, 315°, 270°, and 225°) over the model domain, also described in more detail in Section 3. The results, taken in two transects along the reef edge and nearshore of the project area, shown in Table 3 and Figure 14 below, verified the assumed wave exposure window (270° to 360°) as the directions which produce the greatest wave heights in the project area. It was also determined that longer period waves (15 sec) give higher wave heights on the reef edge as they shoal higher than the shorter period (10 sec) waves.



Figure 14. Location of the two-observation point transects for wave height (Hs) outputs from STWAVE

Table 3. Wave height (Hs) outputs in meters from the directional sensitivity analysis

				Ne	Nearshore Hs [m] at Obs. Pts.					Reef	Hs [m] a	at Obs.	Pts.
idd	wavd	Hs	tp	1	2	3	4	5	6	7	8	9	10
1	45	6.1	10	0.17	0.15	0.17	0.15	0.14	0.13	0.66	1.11	0.72	0.75
2	0	6.1	10	0.17	0.15	0.17	0.15	0.14	0.13	0.66	1.39	0.73	0.75
3	315	6.1	10	0.17	0.15	0.17	0.15	0.14	0.14	0.66	1.39	0.73	0.75
4	270	6.1	10	0.17	0.15	0.17	0.15	0.14	0.14	0.66	1.39	0.73	0.75
5	225	6.1	10	0.18	0.15	0.17	0.15	0.14	0.14	0.50	0.39	0.58	0.75
6	45	49.5	10	0.17	0.15	0.17	0.15	0.14	0.13	0.66	1.25	0.73	0.75
7	0	49.5	10	0.17	0.15	0.17	0.15	0.14	0.13	0.66	1.39	0.73	0.75
8	315	49.5	10	0.17	0.15	0.17	0.15	0.14	0.14	0.66	1.39	0.73	0.75
9	270	49.5	10	0.17	0.15	0.17	0.15	0.14	0.14	0.66	1.39	0.73	0.75
10	225	49.5	10	0.18	0.15	0.17	0.15	0.14	0.14	0.56	0.47	0.67	0.75
11	45	6.1	15	0.17	0.15	0.18	0.15	0.14	0.13	0.66	0.81	0.63	0.76
12	0	6.1	15	0.17	0.15	0.17	0.15	0.14	0.13	0.66	1.41	0.73	0.76
13	315	6.1	15	0.17	0.15	0.17	0.15	0.14	0.14	0.66	1.41	0.73	0.76
14	270	6.1	15	0.17	0.15	0.17	0.15	0.14	0.14	0.66	1.41	0.73	0.76
15	225	6.1	15	0.18	0.15	0.18	0.16	0.15	0.14	0.29	0.19	0.42	0.41
16	45	49.5	15	0.17	0.15	0.17	0.15	0.14	0.13	0.66	0.98	0.71	0.76

17	0	49.5	15	0.17	0.15	0.17	0.15	0.14	0.13	0.66	1.41	0.73	0.76
18	315	49.5	15	0.17	0.15	0.17	0.15	0.14	0.14	0.66	1.41	0.73	0.76
19	270	49.5	15	0.17	0.15	0.17	0.15	0.14	0.14	0.66	1.41	0.73	0.76
20	225	49.5	15	0.18	0.15	0.18	0.15	0.15	0.14	0.37	0.25	0.47	0.53

After confirming the exposure window, an extremal analysis was performed to produce the return wave heights for the project area. A schematic of the wave exposure window is shown in Figure 15. To do this, the WIS dataset was filtered for only those wave directions that were within the exposure window (270° to 360°) and would impact the shoreline of the project area. Then, from the subset of hindcast wave heights they were further filtered by the wave events with wave heights greater than 2 standard deviations above the mean and ranking them highest to lowest. From the resulting ranked list, the return period analysis was performed.

A total of 475 wave heights over the 42-year period match this criterion. The extreme value distribution provides for wave height estimates from 1 to 100-year return period (100 to 1 percent occurrence), shown in Figure 16. The largest recorded wave height within the wave exposure window, 31.2ft. (9.5 m), exceeds the 100-year wave event 28.9ft. (8.8 m), and is associated with Typhoon Pongsona which passed through Guam and CNMI on December 8th, 2002. The 10, 25, and 50-year events were lower, at 19.4ft.(5.9m), 23.3ft(7.1m), and 25.9ft.(7.9m), respectively.



Figure 15. East Hagåtña Wave Exposure Window

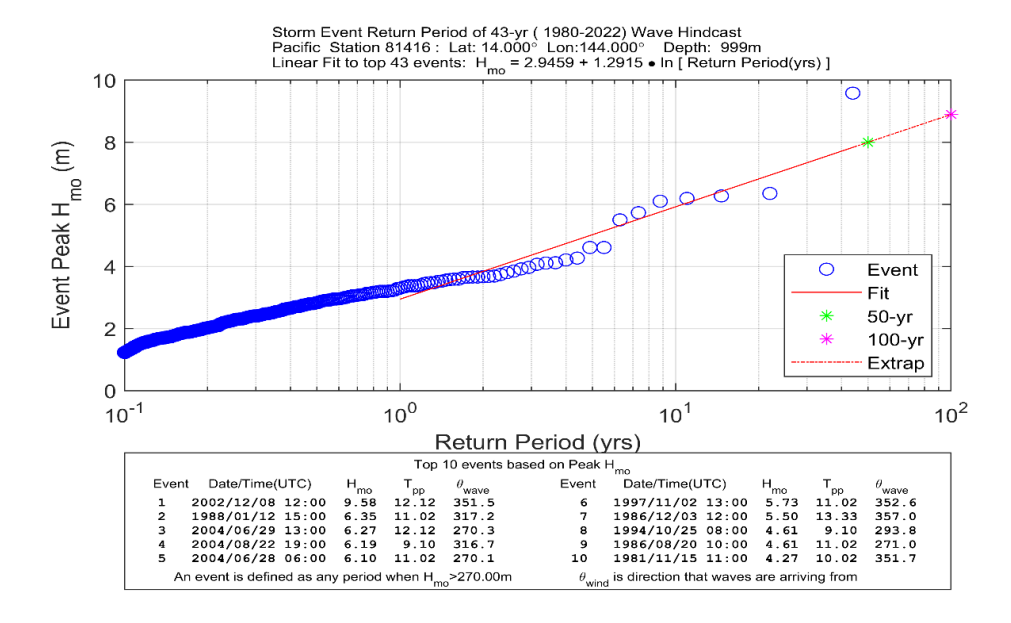


Figure 16. Extremal Analysis for Events within the Exposure Window (270° to 360/0°)

# 2.10. Design Waves & Water Levels

Design wave data was developed by conducting nearshore wave modeling using STWAVE. The water level and wave conditions must be known to supply boundary conditions to the model. The deep-water incident wave conditions used were based on the extremal analysis values (Figure 16), as described in section 2.9.2 above.

Wave height and period are largely independent of one another. That is, a given wave period can have any number of associated wave heights. A limiting factor is that steepness, or the ratio of wave height to wavelength (derived from wave period and water depth), cannot exceed 1/7 otherwise breaking will occur. The return period for wave heights and wave periods can be independently computed and an assortment of combinations of wave heights and periods can be made where each pairing has a 1% annual chance of occurrence. Therefore, another parameter is needed to decide which pairing to use. Since, the formulas for the stability of coastal revetment structures is based largely on wave height. The 10, 25, 50, and 100-year wave heights were combined with periods associated with the longest associated period of similar wave height found in the hindcast record. The longest period was used, as the directional sensitivity analysis confirmed that longer periods produced higher wave heights on the reef edge. In addition, since the top ranked event (Typhoon Pongsona) in the hindcast was higher than the 100-yr wave event, the top ranked event was also included in the model simulations. The mean wave directions were chosen to cover the wave exposure window in 45-degree increments.

Given the shallow nature of the fringing reef, changes in water level can greatly change the nearshore wave action, as deeper water allows for larger wave events to propagate across the reef without breaking. To fully evaluate the effect of water level on wave action at the project area, twelve water level scenarios were used. To represent the elevation of water on the reef from wave's breaking on the reef edge, ponding and setup, were included in all twelve of the selected water level scenarios. Ponding is the increase in water elevation on the reef platform due to offshore waves breaking at the oceanward edge of the reef. Seelig (1983) conducted a

set of laboratory experiments for fringing reefs typical of Guam to investigate hydraulics of reeflagoon systems. He found that the ponding water level is a function of the still water level (astronomical tide and other elevation factors), incident deep water significant wave height and wave period. Gourlay (1996) confirmed these findings. Seelig's equation is as follows:

$$n = a_1 + a_2 \log (H_0^2 T) \tag{1}$$

#### Where.

n=ponding level in m,  $H_0$  is the deep-water significant wave height in m, T is the wave period in sec, and  $a_1$  and  $a_2$  are empirical coefficient dependent on the still water level and wave spectrum (see Table for irregular wave values).

Table 4. Ponding Level Coefficient for Irregular Waves (Seelig 1983)

Depth (m)	$a_1$	$a_2$
0	-0.92	0.77
2	-1.25	0.73

The use of Seelig's calculation's for ponding on the reef was further validated for this study by considering the top ranked event in the extremal analysis (associated with Typhoon Pongona). It was reported that general surge during the event ranged from 10-13 feet (NCEI 2002). Using the average depth of the reef ~4 ft., and the peak water level of the event as measured at Apra Harbor (~3.25 ft.), the calculated ponding resulting from the breaking of the 31.4ft peak wave was approximately 3.2ft. Adding these components together brings the total water level to 10.45ft, which is in the range of increased water levels observed.

While the large offshore waves break on the reef, there is still a significant amount of wave energy which propagates across the reef to shore. These wave heights are limited by the shallow depths of the reef and based on previous research are approximately 0.4 times the local water depth (e.g., Smith 1993). These waves propagate and break nearshore, again elevating the water depth on the reef. The nearshore wave setup was calculated using the Shore Protection Manual's (1984) equation as follows:

$$S_w = 0.15d_b - \frac{\sqrt{g(H_o')^2}T}{64\pi d_b^{1.5}}$$
 (2)

#### Where.

 $S_w$  is nearshore wave setup,  $d_b$  is water depth at breaking over the reef,  $H_o'$  is equivalent normally incident significant wave height over the reef.

Table 5 shows the extrapolated wave heights, periods, and directions from the WIS extremal analysis, and Table 6 shows the associated ponding and setup.

Table 5. Extrapolated Significant Wave heights, Peak Periods, and Mean Wave Directions for use in the numerical model

Event	Significant	Peak Period	Mean Wave
	Wave Height (ft)	(sec)	Direction (deg)
Top Ranked	31.2	12.12	351

10-year	19.4	14	0, 315, 270
25-year	23.3	13	0, 315,270
50-year	25.9	13	0, 315,270
100-year	28.9	13	0, 315, 270

Table 6. Ponding and Setup Calculated for each Wave and Water Level Scenario

Scenario	MSL	MHHW	2%AEP+ MHHW	25low	50low	25int	50int	25high	50high	100low	100int	100high
Top ranked	4.9	4.8	4.6	4.6	4.6	4.6	4.4	4.4	4.2	3.7	4.3	4.5
10-year	3.9	3.8	3.6	3.6	3.6	3.6	3.4	3.4	3.3	2.8	3.3	3.5
25-year	4.3	4.2	4.0	3.9	3.9	3.9	3.8	3.8	3.6	3.1	3.7	3.9
50-year	4.5	4.4	4.3	4.2	4.2	4.2	4.1	4.1	3.9	3.4	3.9	4.1
100- year	4.8	4.7	4.5	4.4	4.4	4.4	4.3	4.3	4.1	3.6	4.2	4.4

The twelve water level scenarios that were identified to investigate the effect of water level on wave action at the project area are described below. The first water level simulated was the MSL datum with no sea level change, in order to provide a lower-bound value of "waves only" for comparison purposes. The second and third water level simulated was representative of present-day water level conditions and included the MHHW (M) water level relative to MSL (+0.97ft) and then MHHW with the linear superposition of the 2% AEP (2A) water level relative to MSL(+2.29ft). The fourth and fifth water levels represented MHHW, the 2%AEP water level and the addition of the low sea level rise curve for 25 and 50 years into the future (M2A25L, M2A50L), +2.8ft and +3.1ft, respectively. The sixth and seventh water levels represented MHHW, the 2%AEP water level and the addition of the intermediate sea level rise curve for 25 and 50 years into the future (M2A25I, M2A50I), +3.1ft and +3.6ft. Similarly, the eighth and ninth water levels represented MHHW, the 2%AEP water level and the addition of the high sea level rise curve for 25 and 50 years into the future (M2A25H, M2A50H), +3.9ft and +6.2ft. Finally, the last three water levels represented the low, intermediate, and high curve for 100 years into the future ((M2A100L, M2A100I, M2A100H)), +3.3ft, +4.9ft, and +9.9ft. The final summary of water levels with the addition of the ponding and setup formulations is shown in Table 7.

Table 7. Design Water Levels in feet

Scenario	MSL	М	2AM	M2A 25L	M2A 50L	M2A 25l	M2A 50I	M2A 25H	M2A 50H	M2A 100L	M2A 100l	M2A 100H
Top Rank	4.9	5.8	6.9	7.4	7.6	7.7	8.0	8.5	9.8	7.1	9.3	14.4
10-year	3.9	4.8	5.9	6.4	6.6	6.7	7.0	7.5	8.9	6.2	8.3	13.4
25-year	4.3	5.1	6.3	6.7	6.9	7.0	7.4	7.8	9.2	6.5	8.7	13.8
50-year	4.5	5.4	6.6	7.0	7.2	7.3	7.7	8.1	9.5	6.8	8.9	14.0
100-year	4.8	5.7	6.8	7.2	7.4	7.5	7.9	8.3	9.7	7.0	9.2	14.3

#### 3. Numerical Modeling

Accurate and representative numerical modeling requires that wave and water level conditions are generally known in deep water, far away from the shoreline and the area of interest. To account for this, the numerical model, STWAVE, was used to transform waves from deep water to the nearshore water depths at the project site. This model has been extensively used thought the United States and the Pacific Ocean, including Guam.

#### 3.1. STWAVE

STWAVE is a phase-averaged spectral wave model for nearshore wave generation, propagation, transformation, and dissipation (Smith et al. 2001, Smith 2007, Massey et al. 2011). Phase-averaging models determine the average conditions over multiple wavelengths. STWAVE numerically solves the steady-state conservation of spectral wave action for the following equation:

$$\sum \frac{S}{\sigma} = \left(C_g\right)_i \frac{\partial}{\partial x_i} \frac{C_g C \cos(\alpha) E(\sigma, \theta)}{\sigma} \tag{3}$$

Where.

i is tensor notation for x- and y- components, Cg is group celerity,  $\theta$  is wave direction, C is wave celerity,  $\sigma$  is wave angular frequency, E is wave energy density, and S is energy source and sink terms. Source and sink mechanisms included surf-zone wave breaking, wind input, wave-wave interaction, whitecapping, and bottom friction.

STWAVE is formulated on a Cartesian grid, with the x-axis oriented in the cross-shore direction (I) and the y-axis oriented alongshore (J), parallel with the shoreline. Angles are measured counterclockwise from the grid's x-axis.

#### 3.2. Model Domain

A single grid was created to transform the incident deep water waves from the WIS station to the nearshore environment at the project area. The model domain was developed using the available 2020 NOAA LiDAR (section 2.6) and a grid cell resolution of 32.8 ft (10 m) to incorporate the fetch and fringing reef characteristics of the area.

The grid was comprised of 180 cells in the cross-shore direction (I) and 325 cells in the alongshore direction (J). The projection of the grid was UTM NAD83 Zone 55 with a vertical datum relative to MSL. The model domain extends north to just below Oka Point, and south to Agana Harbor. The domain stretches west to east about 2 miles. The same domain extents were used to generate a Manning's n friction coefficient grid, with 0.025 representing open water and 0.25 representing the fringing reef.

The properties of the STWAVE domains are provided in Table 8, and the extents are shown in Figure 17.

Table 8. Model Domain Parameters

Projection	Grid Origin (x,y) [m]	Azimuth [deg]	Δx and Δy [ft]	Number Cells	of
.,	L)	լսեցյ			J
UTM					
Zone 55 NAD83	(256013.93,				
MSL	1491713.41)	306	32.8	180	325



Figure 17. STWAVE model domain extents

# 3.3. Offshore Boundary Spectra

The five identified return period wave events (wave height, period, and direction) from Table 4 were used to create a shallow water self-similar spectral form, referred to as a TMA spectrum, which substitutes an expression for the shallow water equilibrium range into the JONSWAP equation for spectral energy density. This spectral form is intended to describe single peaked wind seas, or wind seas which have reached a growth equilibrium in finite depth water. The resolved spectra were represented by 30 frequency bands, ranging from 0.04 Hz (25 sec) to 0.33 Hz (3.03 sec), and 72 directional angle bands, from 0° to 355° with respect to the x- axis (306.0°). Additional offshore inputs included were the twelve selected water elevations from Table 5. The 156 total combinations of wave and water levels that are simulated within the STWAVE model domain are referred to as "idds".

#### 3.4. Model Execution

The STWAVE simulation used the full-plane mode of STWAVE to allow for wave generation and transformation in a 360-degree plane. The full-plane version of STWAVE uses an iterative solution process that requires user-defined convergence criteria to signal a suitable solution. Boundary spectra information is propagated from the boundary throughout the domain during the initial iterations. Once this stage converges, winds and water levels are added to the forcing, and this final stage iteratively executes until it also reaches a convergent state. The convergence criteria for both stages include the maximum number of iterations to perform per time step, the relative difference in significant wave height between iterations, and the minimum percent of cells that must satisfy the convergence criteria (i.e., have values less than the relative difference.) Convergence parameters were selected based on a previous study by Massey et al. (2011) in which the sensitivity of the solution to the final convergence criteria was examined. The relative difference and minimum percent of cells were set as (0.1, 100.0) and (0.1, 99.8) for the initial and final iterations, respectively. STWAVE was set up with parallel in- space execution whereby each computational grid is divided into different partitions (in both the x- and ydirection), with each partition executing on a different computer processor. The number of partitions in the x-direction was 3, while the number of partitions in the y-direction was 5. The maximum number of initial and final iterations was set to a value of 20, higher than the largest partition size.

#### 3.5. Model Outputs

STWAVE transformed the extreme waves and combined water levels discussed in section 2.9. The modeling outputs were analyzed at two transects one nearshore of the project area and one at the reef edge (Figure 14). The output wave heights along the two observation transects, were delineated at every grid cell or every 32.8 ft (10 m).

The reef edge transect gives larger wave heights compared to the nearshore transect per each combination of incident waves and water levels. Figure 18 shows the comparison of wave heights along the transects, for a single selected water level (MHHW + 2%AEP + 50 year of intermediate SLC), for each of the incident wave heights and wave directions. As shown, for a single water level, the greatest variability is found on the reef edge than nearshore. Along the reef edge, the depth and location of the observation point across the transect produces values that can differ in range up to ~1 feet. The reef edge is such a sensitive location due to several interrelated factors. Firstly, wave refraction and diffraction play a significant role as waves approach the reef. Refraction causes waves to bend towards shallower areas, concentrating wave energy in some regions while dispersing it in others, whereas diffraction occurs when waves encounter the reef itself, leading to wave spreading. Additionally, the variations in water depth are crucial; as waves travel over deeper waters, they retain their energy, but as they move into shallower areas near the reef, they slow down and increase in height due to the shoaling effect. The physical structure and topography of the reef, including its contours, ledges, and gaps, further influence the wave behavior. Waves may break over the crest of the reef, losing energy and height, while in other areas, the existence of slight to deeper channels allow waves to pass through with less energy loss. Not captured in the model bathymetry but important to note that localized reef features like coral heads, sandbanks, and boulders can also focus or disperse wave energy, leading to variations in wave heights along the reef edge.

In contrast, the nearshore observation points along the transect give values that differ less than 0.2ft. The nearshore area experiences more consistent wave action because, as waves moves into the shallower, more uniform depths, their energy becomes more evenly distributed. The

reef acts as a barrier, absorbing and dissipating much of the wave energy, resulting in smaller and more uniform waves reaching the shore. Additionally, the bathymetry nearshore is generally more consistent with fewer areas of complex topography, which would otherwise contribute to wave refraction, diffraction, shoaling and localized energy focusing. This uniformity leads to more stable and predictable wave patterns.

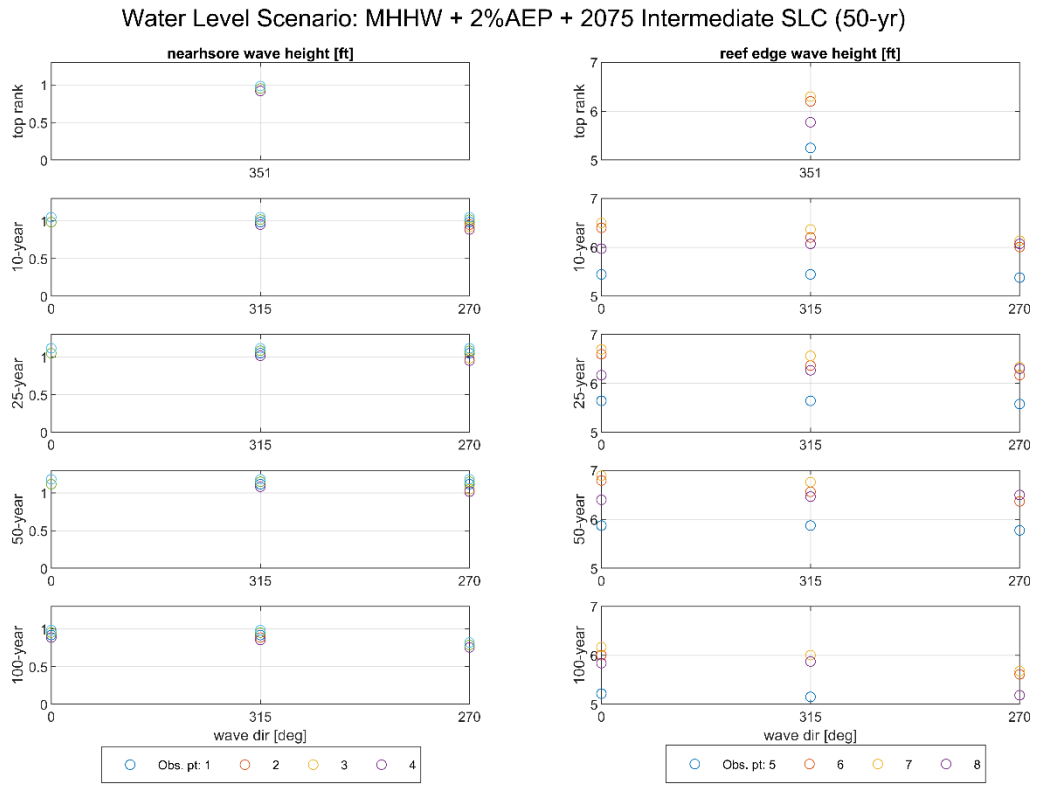


Figure 18. Observed wave heights along the reef edge an dnearshore transects for a single water level scenario

Figure 19 and Figure 20, give another look at the resulting wave heights along the two transects by showing the outputs over the various water level scenarios. It is shown that both the observed significant wave heights along the reef edge transect, Figure 19, and the nearshore transect, Figure 20, are the most impacted by significant increases in water level. This is congruent with the fact that higher water levels allow waves to pass over the reef crest with less obstruction, maintaining more of their energy and height. When water levels are higher, the increased depth reduces the frictional drag exerted by the reef's surface on the waves, allowing them to travel with greater force and height. Conversely, at lower water levels, the reef is more exposed, causing waves to break earlier and lose significant energy, resulting in reduced wave heights. Thus, the depth of water over the reef directly correlates with the height of the waves observed. As such, there is a small increase in wave height when the water level increases during the MHHW+2%AEP+50 years in the future high SLC and the MHHW+2%AEP+100years in the future high SLC (MA50H and MA100H). The maximum significant wave height on the reef edge and nearshore for all water levels was consistently associated with the offshore wave event representative of the Top ranked event.

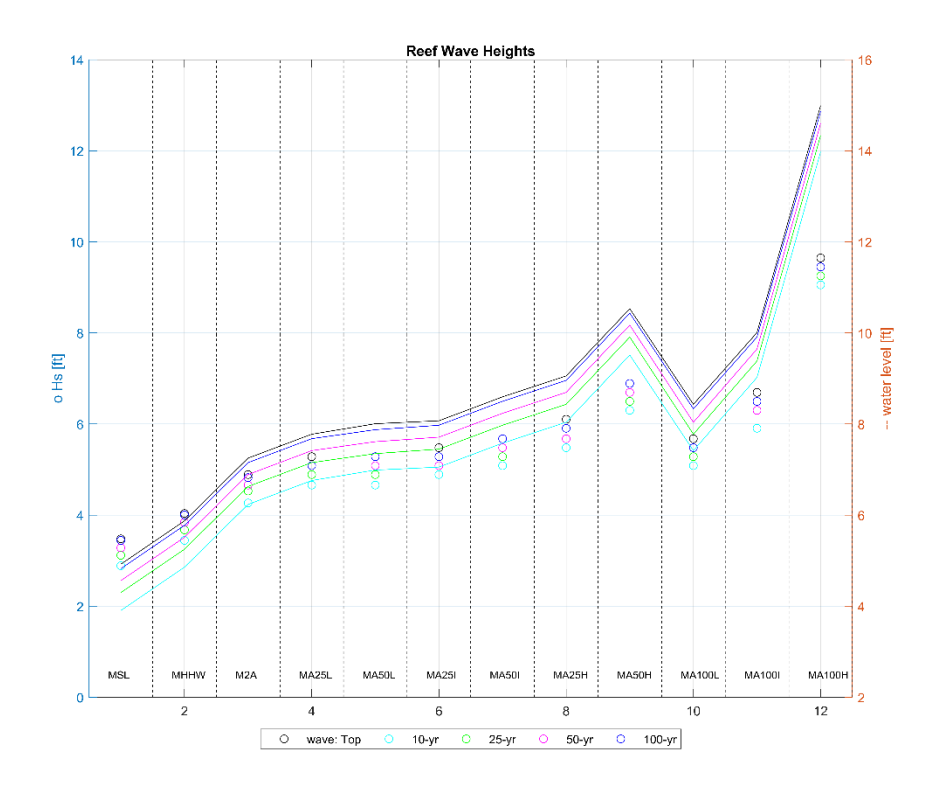


Figure 19. Maximum model outputs along the reef edge transect, Significant wave height in feet is shown on the left y-axis, and water elevation (feet) is shown on the right y-axis.

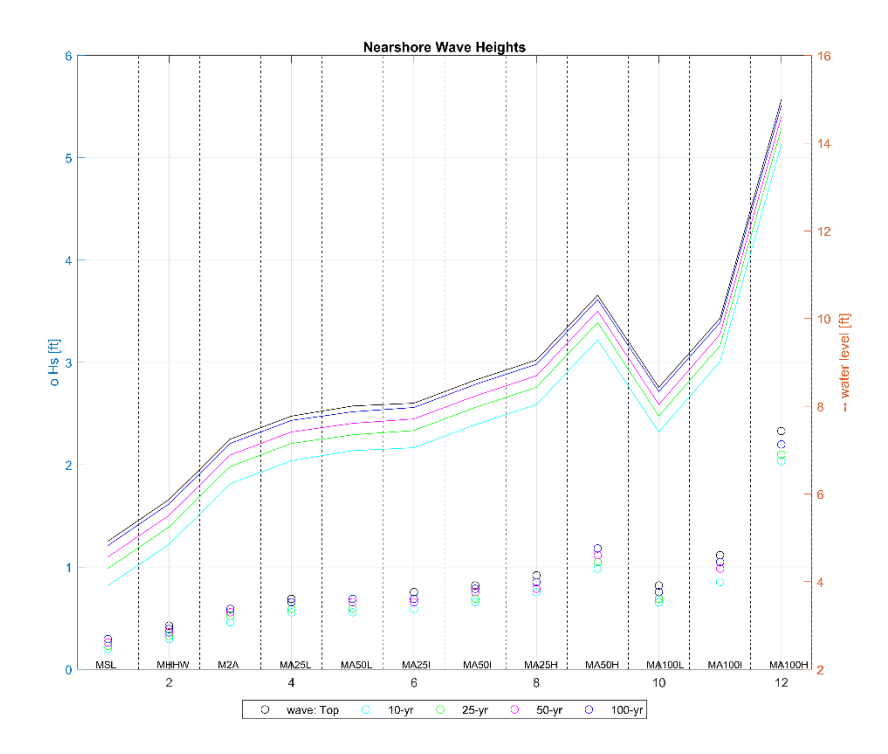


Figure 20. maximum model outputs along the nearshore transect, Significant wave height is shown on the left y-axis, and water elevation is shown on the right y-axis.

For use in design of the alternative measures, described in more detail in section 4, wave height and water level values need to be identified. To do this, the maximum wave height value observed for each water level scenario along both transects were extracted. As the bathymetry is inherently representative of the "without project" conditions, the depth limited wave height at the assumed toe of the proposed alternatives (i.e. no sand or other covering over limestone) as described in section 4, was also computed for comparison. The depth limited wave height was determined from the assumed depth of the limestone (-2.6ft) at the project area from the LiDAR surveys (Section 2.7) and the depth of water associated with each water level scenario. The final array of potential wave heights for design are summarized in Table 9.

Table 9. Final Array of Design Wave Heights Per Water Level Scenario.

Water Level Scenario	Offshore Wave Height (ft)	Water Level (ft relative to Toe)	Depth Limited Wave height above Toe (ft)	Nearshore Max Wave Height (ft)	Reef Edge Max Wave Height (ft)
MSL	31.2	7.5	3.01	0.31	3.49
М	31.2	8.4	3.34	0.42	4.05
M2A	31.2	9.5	3.81	0.61	4.90
M2A25L	31.2	10.0	3.98	0.70	5.28
M2A50L	31.2	10.2	4.06	0.70	5.28
M2A25I	31.2	10.3	4.10	0.76	5.49
M2A50I	31.2	10.6	4.25	0.81	5.69

M2A25H	31.2	11.1	4.42	0.93	6.09
M2A50H	31.2	12.4	4.97	1.19	6.89
M2A100L	31.2	9.7	3.89	0.81	5.69
M2A100I	31.2	11.9	4.76	1.12	6.69
M2A100H	31.2	17.0	6.80	2.32	9.64

There is little variability between the M2A50L, M2A50I, M2A50I, and M2A100L water levels and corresponding transect wave heights, however as shown in Section 2.8.2. and Figure 12 the intermediate SLC curve aligns with the recently observed water level trend records at the Apra Harbor Gauge. Therefore, the M2A50I, water level was chosen for design. The depth limited wave height of 4.25 ft. was also selected as it represents exposed limestone, a conservative condition possible over the next 50 years. The use of the depth limited wave height avoids underestimating wave heights at shallower nearshore points that might see increased exposure if the sand cover erodes, while conversely, it prevents overestimation at the reef edge, where large offshore waves break but are less relevant to the nearshore conditions. By moving forward with the depth-limited wave height approach, the study simplifies the analysis while directly addressing the critical concern of future reef exposure. This approach is conservative in nature, ensuring that assessments prioritize preparing for potential increases in wave impacts due to erosion.

Figures of the wave fields from each idd of the model simulation are in the Model Output Appendix.

# 4. Engineering Alternatives

# 4.1. Preliminary Array of Measures

To develop preliminary costs and layouts to assist project analysis for other disciplines, a preliminary array of measures consists of:

- 1. No action
- 2. Revetment
- 3. Precast Concrete Wall
- 4. Concrete Rubble Masonry (CRM) Wall
- 5. Secant Wall
- 6. Permeation Grouting
- 7. Beach nourishment

Descriptions and details of all the measures are provided in the following sections. However, the Secant Wall, Permeation Grouting, and Beach Nourishment measures were screened out for costs of equipment, labor, and materials (details of the screening are provided within their section). The no action, revetment, precast concrete wall, and Concrete Rubble Mason Wall measures were carried forward, with the precast concrete wall as the tentatively selected least cost environmentally acceptable plan.

#### 4.2. No Action

The no action alternative assumes the existing conditions would continue unchanged into the future. This alternative would not include shoreline protection or stabilization. Erosion would continue and the shoreline will approach Marine Corps Drive. This would eventually lead to undermining and failure of the existing wall and ultimately damages to roadway.

#### 4.3. Revetment

A revetment consists of armoring a shoreline slope designed to hold-the-line (Figure 21) and protect the shoreline slope from wave impacts and erosion. A revetment is suitable in areas of pre-existing hardened shorelines and in some cases along chronically eroding shorelines with limited sediment supply. It may also be appropriate where shoreline recession threatens infrastructure that is not able to be relocated. Materials that are commonly used in revetment construction include stone, concrete armor units, sand/concrete filled geotextile bags, geotubes, and rock-filled gabion baskets.

Revetments mitigate wave action, there is limited maintenance, and have an indefinite lifespan. Disadvantages however include significant land area requirement, loss of intertidal habitat, erosion of adjacent unreinforced shoreline, limited high water protection, and prevention of the upland from being a sediment source to the system. Environmental considerations include large impact in and out of water, impacts are not reversible, minimal maintenance required, and permits are required.

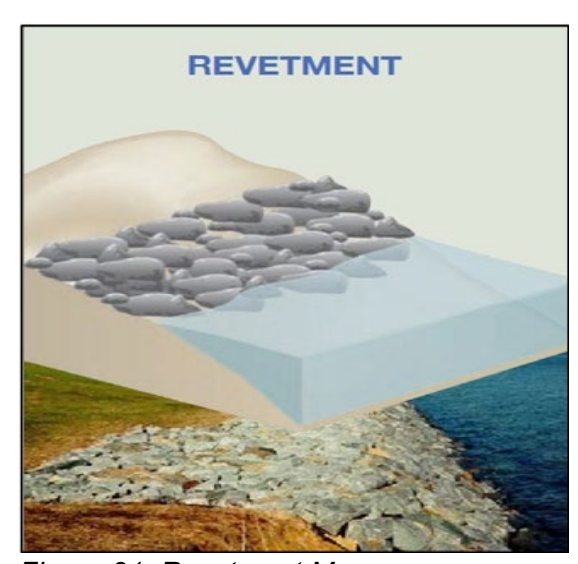


Figure 21. Revetment Measure

Revetments were determined to be an acceptable option for the East Hagåtña shoreline. Two different materials for the armor layer of the revetment were considered, rock and concrete armor units. Both materials have been used successfully to protect critical infrastructure such as roadways. Contractors on Guam are most familiar with rock revetments, but an increasing number of tribar, a type of concrete armor unit, revetments have been implemented on other islands in the CNMI. Revetments can be completed without specialized equipment. Both a rock revetment and tribar revetment were carried forward into the final array of alternatives, so that armor unit size, availability, cost, and environmental impacts could be fully evaluated. However, ultimately the tribar revetment was determined as the final design, as queries to the local quarries on Guam, showed a threshold of stone sizing at 500 lbs, which is smaller than the stone size needed as described in the following sections.

The revetment design for either material (rock or tribar) was created as to replace the existing seawall and extend seaward. The proposed revetment footprint is shown in Figure 22.

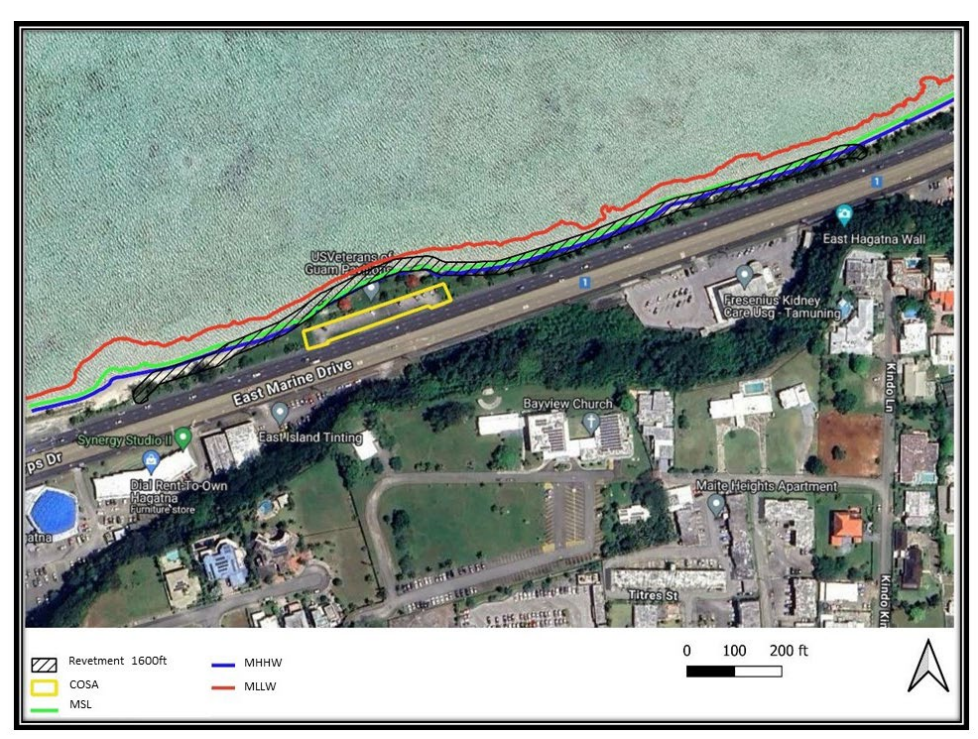


Figure 22. Revetment Preliminary Footprint

#### **Design Considerations**

Although the design was not optimized to reduce runup and overtopping from future sea level rise scenarios, estimates of runup and overtopping were calculated to evaluate the performance of the alternative, as runup and overtopping can result in backshore erosion. Wave runup and overtopping are complex physical processes occurring in the surf and backshore zones where waves encounter the shoreline and break, resulting in an uprush of water. They depend on the local water level, incident wave conditions, and the nature of the beach or structure encountered.

The lidar determined topographic and bathymetric elevations and depths were used to inform the crest elevations of the revetment and the other proposed structural alternatives. The limestone is assumed to be at approximately -2.6 ft. MSL and the existing wall crest at +8.9 ft. MSL, for a total structural height of approximately 12 ft. computed runup and overtopping.

To compute runup, equations 5.1 and 5.2 from the EurOtop Manual (2018) were used, which describes runup as:

$$\frac{R_{u2\%}}{H_{m0}} = 1.65 * \gamma_b * \gamma_f * \gamma_\beta * \xi_{m-1,0} \tag{4}$$

with a maximum of

$$\frac{R_{u2\%}}{H_{m0}} = 1.0 * \gamma_f * \gamma_\beta (4 - \frac{1.5}{\sqrt{\gamma_b * \xi_{m-1,0}}})$$
 (5)

where, Ru2% is the wave run-up height exceeded by 2% of the incoming waves,

Hm0 is the incident significant wave height,  $\gamma b$  is the influence factor for a berm,  $\gamma f$  is the influence factor for roughness elements on a slope,  $\gamma \beta$  is the influence factor for oblique wave attack and  $\xi m-1,0$  is the breaker parameter.

Overtopping was calculated using equations 5.10 and 5.11 from the EurOtop Manual (2018):

$$\frac{q}{\sqrt{g * H_{m0}^3}} = \frac{0.023}{\sqrt{\tan \alpha}} \gamma_b * \xi_{m-1,0} * \exp\left[-\left(2.7 \frac{R_c}{\xi_{m-1,0} * H_{m0} * \gamma_b * \gamma_f * \gamma_\beta * \gamma_v}\right)^{1.3}\right]$$
 (6)

with a maximum of

$$\frac{q}{\sqrt{g * H_{m0}^3}} = 0.09 * \exp\left[-\left(1.5 \frac{R_c}{H_{m0} * \gamma_f * \gamma_\beta *}\right)^{1.3}\right]$$
 (7)

where, q is the overtopping rate,  $[\![H]\!]$  \_m0 is the incident significant wave height,  $tan [\![H]\!]$  as the structure slope,  $tag{\gamma}_{-}(b)$  is the influence factor for a berm,  $tag{\gamma}_{-}(b)$  is the influence factor for oblique wave attack,  $tag{\gamma}_{-}(b)$  is the influence factor for oblique wave attack,  $tag{\gamma}_{-}(b)$  is the influence factor for a wall at the end of a slope,  $tag{\zeta}_{-}(b)$  is the breaker parameter, and  $tag{\zeta}_{-}(b)$  is the freeboard.

Under the design water level of 10.6 ft relative to the toe of the structure (8.1 feet relative to MSL), which represents MHHW+2%AEP+50years of SLC intermediate curve + ponding and setup of the top ranked event on the reef (M2A50I) as described in section 2.10, the project area would be almost submerged (total structure height of 12 feet). Therefore, to evaluate overtopping and runup, an analysis of the sensitivity to water level as it relates to runup and overtopping for structure stability was performed.

This was completed by increasing the water level in 1-foot increments starting at MHHW + 2%AEP with ponding and setup from the 10-year incident wave event relative to the toe of the structure (8.5ft). The decision to use the 10-year ponding and setup was in an effort to evaluate the structure without submergence, and also evaluate the structure under the more frequent occurring high water levels present day. The depth limited wave height of each water level increment was used, and both rock and tribar were included in the analysis. For rock, it was assumed that the revetment was composed of 2-layers of stone with an impermeable core, setting the roughness coefficient,  $\gamma f$ , to 0.55 per the EurOtop Manual Table 6.2. Similarly, for tribar, the roughness coefficient was set to 0.44. The results of this analysis are summarized in Table 10.

Table 10. Runup and Overtopping Rates under Water Levels

Water Level Depth (ft):	8.5	9.5	10.5	11.5
Depth limited wave height (ft.)	3.40	3.80	4.20	4.60
peak period (s)	12	12	12	12
Rock				

				l I	
Runup (ft)	6.54	7.28	8.02	8.75	
Overtopping (ft^3/s/ft)	0.36	1.43	3.58	6.12	
Overtopping (m^3/s/m)	0.03	0.13	0.33	0.57	
Tribar					
Runup (ft)	5.23	5.83	6.41	7.0	
Overtopping (ft^3/s/ft)	0.17	1.03	3.34	6.1	
Overtopping (m^3/s/m)	0.02	0.10	0.31	0.57	

As shown, due to the greater friction of the tribar, it performs better for runup and overtopping with lower rates than those observed for rock. Overall, runup ranged from 5.1ft to 8.6ft, and overtopping from 0.11 ft^3/s/ft to 5.41 ft^3/s/ft. The water level sensitivity analysis shown, an inflection point beginning around the 9.5 foot water depth results in significantly larger amounts of overtopping for both rock and tribar. As shown in Figure 21 from the Engineering Manual 1110-2- 1100 Part VI, the critical values of overtopping rates for a revetment, are 0.54 cfs/ft (50 liters/s/m) if unpaved, and 2.1 cfs/ft (200 liters/s/m) for paved. As such, it was determined that paving the promenade behind the crest of the revetment is a preventative measure for the structure's stability under wave events. Additionally, as sea level rises in the future and offshore wave events grow stronger producing ponding and setup on the reef, overtopping events will become more frequent and more severe, indicating that monitoring of the structure's stability and continual assessments of the crest elevation will be needed. The crest of the structure for either rock or tribar can be raised through measures such as adding additional layers of armor units/rocks or by adding a CRM wall built behind the crest of the structure.

Runup and overtopping analysis was also conducted for the vertical wall alternative measures such as the precast concrete wall, concrete rubble masonry wall, and secant wall for which the designs are discussed in detail in Sections 4.5 through 4.7.

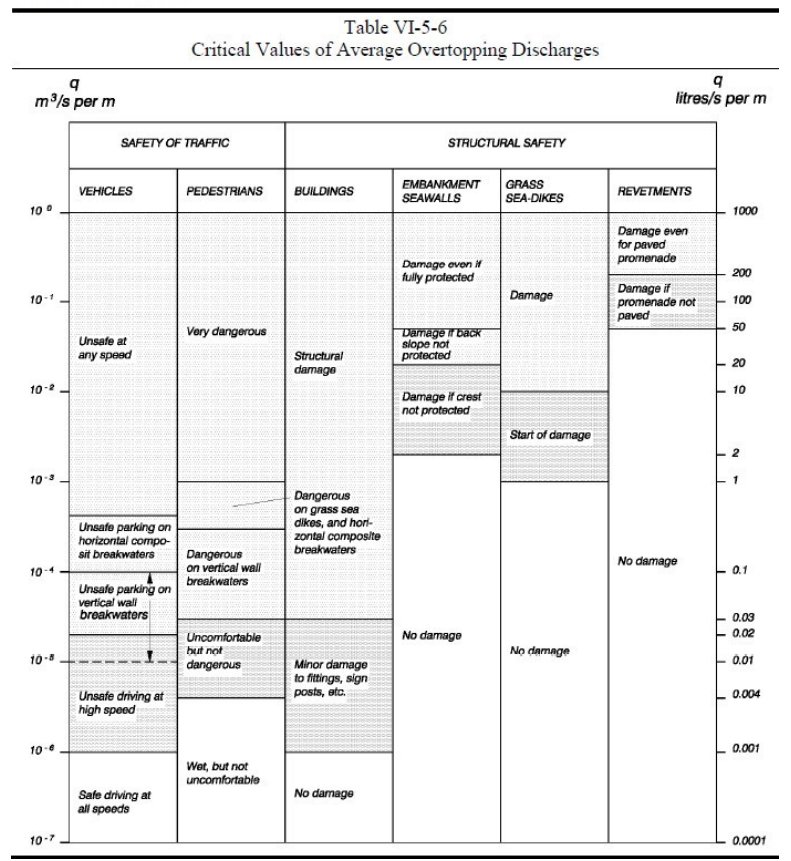


Figure 23. Critical Values of Overtopping Discharges

# Preliminary Design

#### Rock

The site-specific revetment design is typical for such a structure and is shown in Figure 22. The structure consists of two layers of armor stone, and two layers of underlayer stone, which sit on top of compacted backfill and a geotextile layer. All of which are secured by an oversized toe stone. The crests elevation is expected to be +8.9 feet (MSL), the assumed elevation of the existing structure, as discussed in section 2.7. The toe will be situated in a trench excavated approximately 1-2 feet into the limestone, at a depth of -3.6 ft (MSL). The structure crest elevation and toe depth may need to be adjusted due to natural variations in the ground elevations along the project length. The revetment would replace the existing sea wall, with the crest of the revetment aligned with and replacing the crest of the existing wall.

The armor stones form the outermost layer and dissipate energy to provide protection from waves and water levels along the structure. The Hudson Equation, as shown below, was used to determine the appropriate stone sizing of the armor stones.

$$W = \frac{\gamma_r H^3}{K_D (S_a - 1)^3 cot \alpha} \tag{11}$$

Where, W is the weight of the required armor stone, yr is the specific weight of the armor units,

H is the design wave height,  $K_D$  is the damage coefficient,  $S_a$  is the specific gravity of the armor stone, and cot $\alpha$  is the angle of the breakwater side slope. The  $K_D$  value was selected based upon rough angular stones and random placement for breaking waves.

The underlayer is added to support the armor layer such that the armor stones are not directly resting on the geotextile fabric. The underlayer is designed in accordance with the USACE's Coastal Engineer Manual (CEM); the weight of the underlayer stone is 1/10 of the armor layer stones. This size requirement prevents underlayer stones from escaping through voids in the armor layer.

The toe stone is the seaward terminus of the structure and provides stability to the structure. Typically, these are sized on the order of one and a half times the armor stone (CEM). Likewise, the splash apron is the landward terminus of the structure and provides stability to the structure from backshore erosion.

Table 11 provides the assumed variables and coefficients used in the Hudson Equation calculations and the resulting stone sizing. Queries to the local quarries on Guam, revealed a threshold of available stone size to be approximately 500 pounds (0.25 tons). As such, the design of the revetment was pivoted for the use of concrete armor units.

Specific Weight (γr) (lbs/ft3)	154	Median Armor Weight (tons)	0.8
Stability Coefficient (KD)	2	Median Armor Diameter (ft)	2.1
Sideslope Angle ( $\cot \alpha \alpha$ )	1.5	Underlayer Weight (tons)	0.08
Design Water Level relative to the toe (ft)	11.2	Underlayer Diameter (ft)	1
Design Wave Height (ft)	4.25	Toe Weight (tons)	1.2
Specific Gravity (Sa)	2.4	Toe Diameter (ft)	2.6
Layers	2		

#### Tribar

Due to an approximate 500 lbs. threshold of available stone on Guam, concrete armor units were considered. Concrete armor units function as the armor layer within the revetment. There are many different designs of concrete armor units available today, such as COR-LOCK, Dolos, cubes, tribar, tetrapods and many others. Each design has been well tested with slight differences in shape for better performance under various scenarios. For the East Hagatna project area tribar was selected for its compact interlocking and turning radius, and the higher likelihood of available and experienced contractors with the design.

A tribar revetment would be constructed like the rock revetment with the structure parallel to the shoreline and replacing the existing wall. The design considerations for the tribar revetment were a length of 1630 ft, alignment with the existing wall, a crest elevation of +8.9ft and bottom

elevation of -3.6ft, and a slope of 1.5V:1H. An example of a typical tribar unit and a visual of this type of material implemented in Saipan, CNMI is shown in Figure 24.

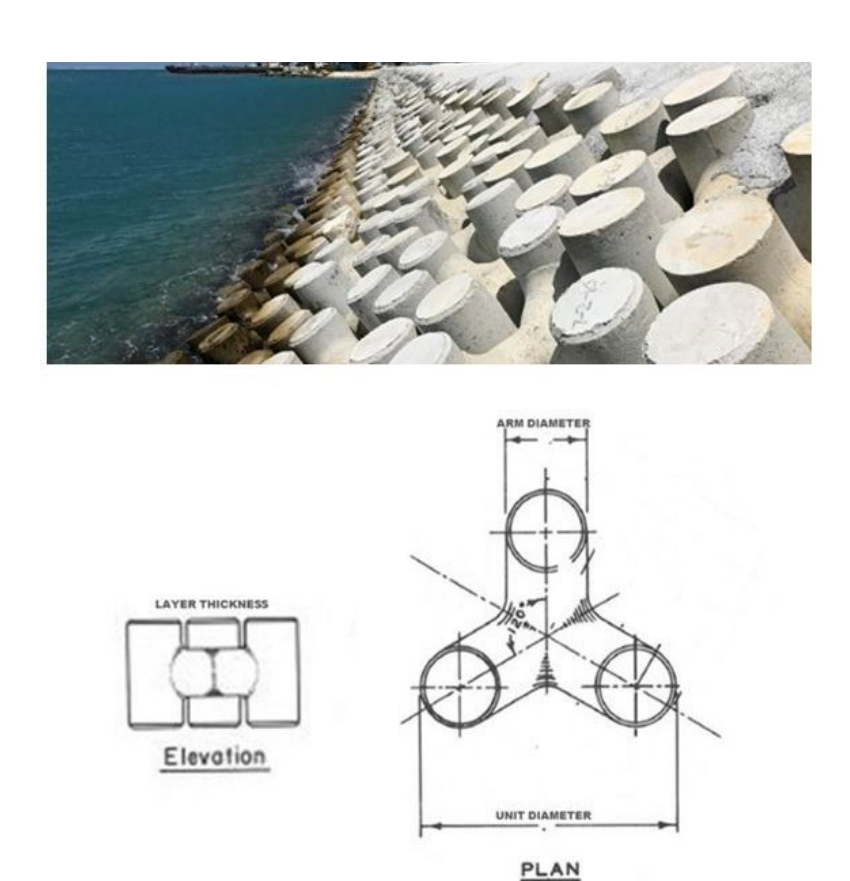


Figure 24. Example of typical tribar unit and visual air form a project in Saipan.

The tribar units would be placed in a single layer, uniformly, as is typical for this type of design. The toe Tribar unit would be cemented at the toe, and grout filled geotextile bags would serve to seal the crest (6.5ft wide) with a splash apron composed of formed concrete over a gravel fill (3 ft wide). An example Tribar cross section is shown below in Figure 25. Using design equations similar to the rock revetment design (i.e. Hudson equation), a less than 1-ton weight was designed for (0.7 tons) however a design for 1-ton was chosen for the area, due to fragility concerns of smaller than 1-ton tribar units, and because 1-ton is the more common and consequently more available size form. The 1-ton unit has an individual arm diameter of 1.3 ft., a unit diameter of 4.1 ft., and an average layer thickness of 2.7 ft. Example schematics of 1-ton Tribar units are shown below in Figure 26. The underlayer stone would be approximately 10% the size of the Tribar, to prevent the material from escaping through the openings. All weights and diameters and other metrics for the Tribar units are summarized in Table 9.

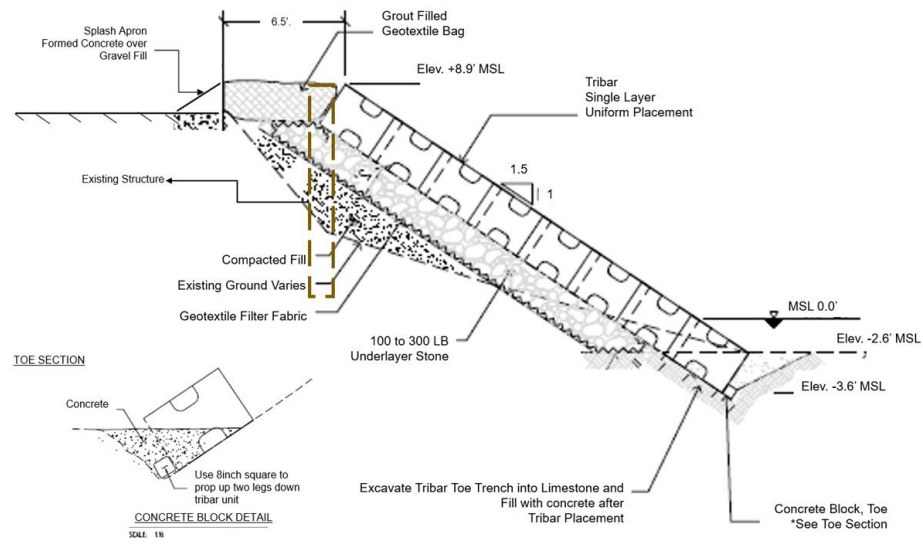


Figure 25. Preliminary Tribar Revetment Cross Section

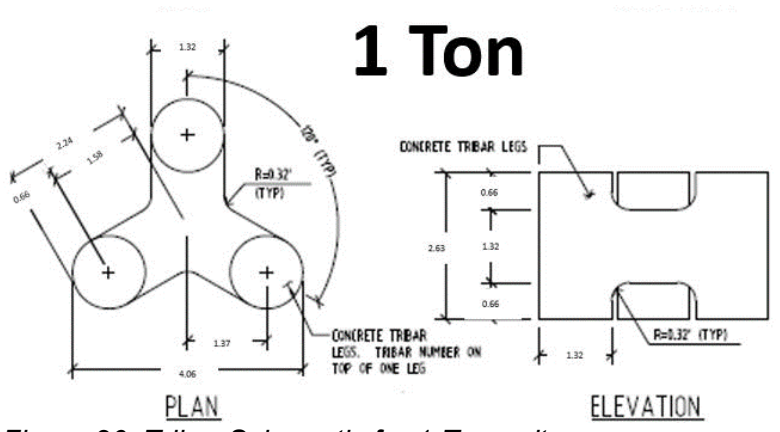


Figure 26. Tribar Schematic for 1-Ton units

Table 12. Additional tribar sizing values

Volume of individual armor units (cu ft)	14.29
Weight of individual armor unit (ton)	1
Unit Weight LB/Cu ft	140
Average measured thickness (1layer uniform) (ft)	2.74
Number of armor units per 1000 sq ft (1layer uniform)	101.63 (4620 units)
Tribar arm diameter (ft)	1.3
Tribar unit diameter (ft)	4.1
Layer Thickness (ft)	2.7

# Construction and Maintenance

Construction of the tribar revetment would be conducted with the use of conventional landbased earth moving equipment. The existing wall would be removed, and the revetment would be constructed from the toe to the crest elevation. To provide stability to the toe of the structure, a 1-2 ft trench would be excavated into the limestone with an 8-inch concrete block placed flushed into the bottom of the trench which will prop up the terminal unit and then be sealed by a concrete fill. The tribar units have fixed dimensions and are placed directly on top of each other in sloped rows. Careful placement during construction will ensure that units properly interlock, units are not damaged during placement, and that design dimensions are met. To accommodate the thickness of the structure, the ground elevation will need to be excavated approximately 1-2 ft to accommodate the crest elevation of the structure (+8.9ft MSL). A splash apron composed of formed concrete over a gravel fill behind the crest of the structure will tie the structure to the existing ground. Excavated material can be used to backfill the beach in front of the structure, or on the ends fronting the tie backs. The final footprint would be approximately 28 ft. wide (18 ft sloped structure +6.5 ft crest + 3 ft splash apron). The total structure height is approximately 12.5 ft. from toe to crest (-3.6 ft to +8.9 ft MSL), with the crest of the revetment aligned (and replacing) the crest of the existing wall.

A tribar revetment typically requires less maintenance than a rock revetment when the structure is damaged and in need of repair. Common types of damage include broken units, loss of underlayer material, and flanking. The extent of damage will dictate the need for repairs.

#### Adaptive Management

Adaptation measures for the revetment alternatives, to provide adequate shoreline protection within the 100-year adaptation horizon should be considered. Water Levels for the three SLC curves were evaluated, and under the high and intermediate curves, the structure and surrounding area will be submerged. Under the low curve the proposed structure will be submerged only under 100-year events or greater. Therefore, as sea level change continues into the future, the project area will experience more severe and frequent overtopping and will need increases in monitoring of the structure as well as the potential adaptations discussed in the design consideration section.

### 4.4. Vertical Seawall Measures

Differing from the sloped design of the Revetment, the following alternatives (sections 4.5 through 4.7) are vertical in nature. The vertical wall alternatives, or seawalls, are constructed parallel to the shoreline and function as rigid, vertical or near vertical retaining walls (Figure 27). They are intended to hold soil in place, survive the impacts of waves/currents and provide for a stable shoreline. Suitable applications are in high energy settings and sites with pre-existing hardened shoreline structures. These types of structures are commonly used along bay and ocean shorelines. The material options include various types of sheet pile, grouted rock, and prefabricated or cast in place concrete elements. Advantages of the seawall measures include prevention and/or reduction of storm surge flooding, resistance to strong wave forces, shoreline stabilization behind the structure, low maintenance costs, and a limited footprint.

Disadvantages include potential erosion in front or to ambient shorelines of the structure due to wave reflection, disruption of sediment transport leading to beach erosion, higher up-front costs, visually obstructive, loss of intertidal zone, prevention of upland from being a sediment source to the system and may be damaged from overtopping. The vertical or near vertical property of these measures creates an increase in runup and overtopping compared to the sloped revetment (~0.4 ft) as the waves are not able to dissipate energy over a slope. They can cause relatively large environmental impacts in and out of the water, impacts may not be reversible, there is minimal maintenance, and permits are required. The vertical measures proposed in the following sections include a precast concrete wall, a rubble masonry wall, and a secant wall.

Additional details on the design of the vertical walls is located in the A.2 Geotechnical Appendix.

Runup and overtopping analysis was conducted for the vertical wall alternative measures such as the precast concrete wall, concrete rubble masonry wall, and secant wall for which the designs are discussed in detail in Sections 4.5 through 4.7. The results of this analysis are shown in Table 13. Inputs were similar to those discussed in section 4.3 for the revetment, with changes to the roughness coefficient to a value of 1, for a smooth impenetrable surface and a structure slope of 0°. Given that overtopping on vertical structures has a lower critical threshold (0.54 cfs/ft) than a revetment (2.1cfs/ft) (Figure 23), while also incurring higher values for runup and overtopping, a paved promenade or splash apron will be included in the design of all of the vertical structures, and it is strongly recommended that monitoring and continual assessment of the structure is conducted to allow for the timely identification and remediation of any weaknesses or damage caused by changing conditions and extreme weather events.

Water Level Depth	8.5	9.5	10.5	11.5
Depth Limited Wave Height (ft)	3.40	3.80	4.20	4.60
Peak Period (s)	12	12	12	12
Runup (ft)	13.16	14.69	16.23	17.76
Overtopping (cfs/ft)	1.17	2.42	4.0	6.12

0.11

0.23

0.37

0.57

Table 13. Runup and Overtopping values for various water levels



Figure 27. Vertical Wall Measure (Seawall)

Overtopping (m3/s/m)

### 4.5. Precast Concrete Wall (Tentatively Selected Plan)

The proposed precast concrete wall acts as a cantilever retaining wall. These types of cantilever retaining walls utilize the weight of the backfill to provide resistance to the lateral earth pressures. The precast concrete panel wall consists of individual concrete panels that are installed throughout the length of the project. This type of structure provides adequate structural stability with the buried reinforced section of the panel wall and adequate overtopping protection from the crest elevation. The footprint of the precast concrete wall is shown in Figure 28.



Figure 28. Precast Concrete Wall Preliminary Footprint

### **Design Considerations**

The proposed precast concrete wall acts as a cantilever retaining wall. These types of cantilever retaining walls utilize the weight of the backfill to provide resistance to the lateral earth pressures. The precast concrete panel wall consists of individual concrete panels that are installed throughout the length of the project. This type of structure provides adequate structural stability with the buried reinforced section of the panel wall and adequate overtopping protection from the crest elevation.

The preliminary design also includes a set of concrete stairs, approximately 4-5 feet wide, running parallel to the wall to maintain continued access to the beach. Additionally, weep holes are included to ensure proper drainage.

### **Preliminary Design**

This design of the Precast Concrete Wall is as follows. The wall will be constructed of precast concrete panel units. The panels can be cast either on-site or cast off-site and transported to the site. Existing conditions indicate a natural limestone bench at -2.6 feet (MSL) on top of which the panels would sit. This structure relies upon the weight of the structure, and the weight of the earth on top of the buried section to prevent sliding, overtopping due to rotation and resistance to wave forces. Placement would replace the existing seawall.

The concrete panels were determined to be approximately 1 ft. thick and would extend upward from the existing ground level at the limestone bench (-2.6 ft MSL) to +8.9 ft. (MSL). The buried panel section would extend landward 7 ft. and the entire panel would be no less than 1 ft. thick. To place the panels, the ground will need to be excavated and graded at a distance of approximately 20-30 feet. In the areas where the project is limited in extent, such as near the park pavilion structures or the west end of the park, excavation will be appropriately limited by increasing the slope and using reinforcements as necessary. A typical cross section of the

precast concrete wall is shown in Figure 29. For more detailed descriptions of the presented alternative refer to the Geotechnical Appendix A.2.

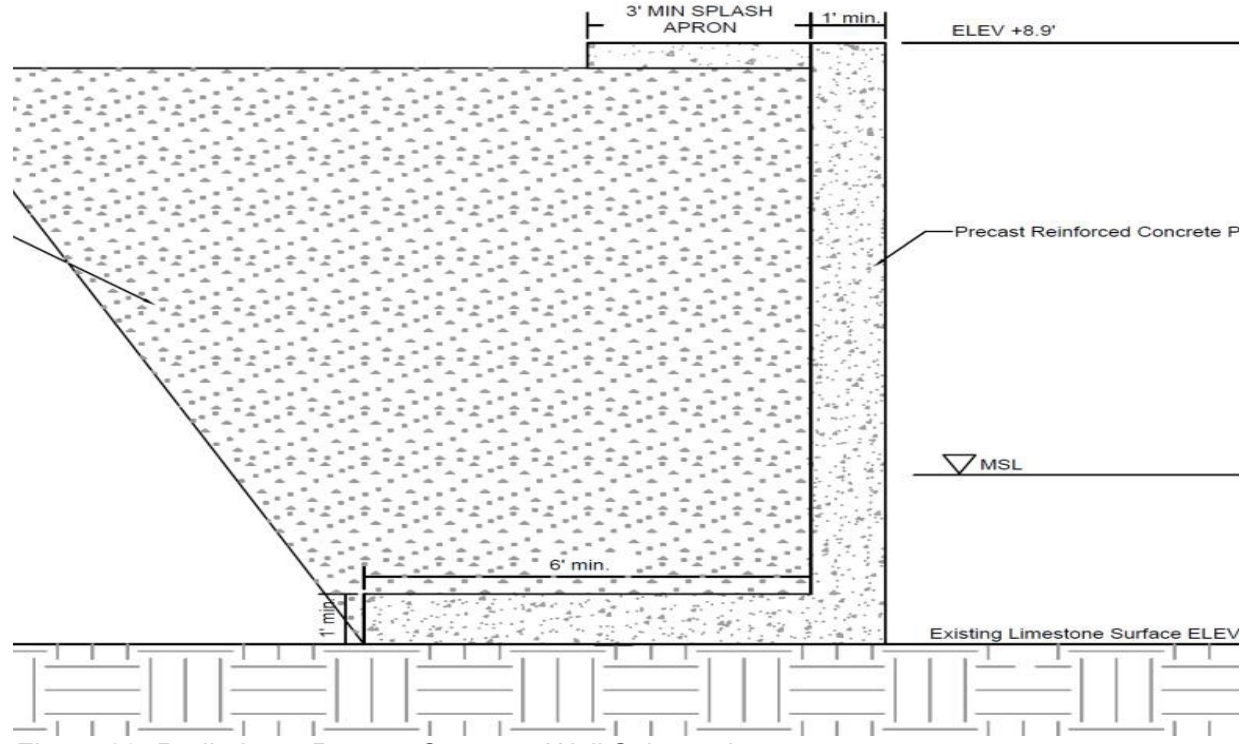


Figure 29. Preliminary Precast Concrete Wall Schematic

# 4.6. Concrete Rubble Masonry Wall

A concrete rubble masonry (CRM) wall consists of a CRM wall bearing on a reinforced concrete foundation. The CRM wall would be a vertically oriented structure generally shore-parallel along the shoreline to protect from overtopping due to waves and water levels and to fix the shoreline so erosion cannot occur landward. CRM walls are typical structures used throughout the area. The CRM wall footprint is shown in Figure 30.

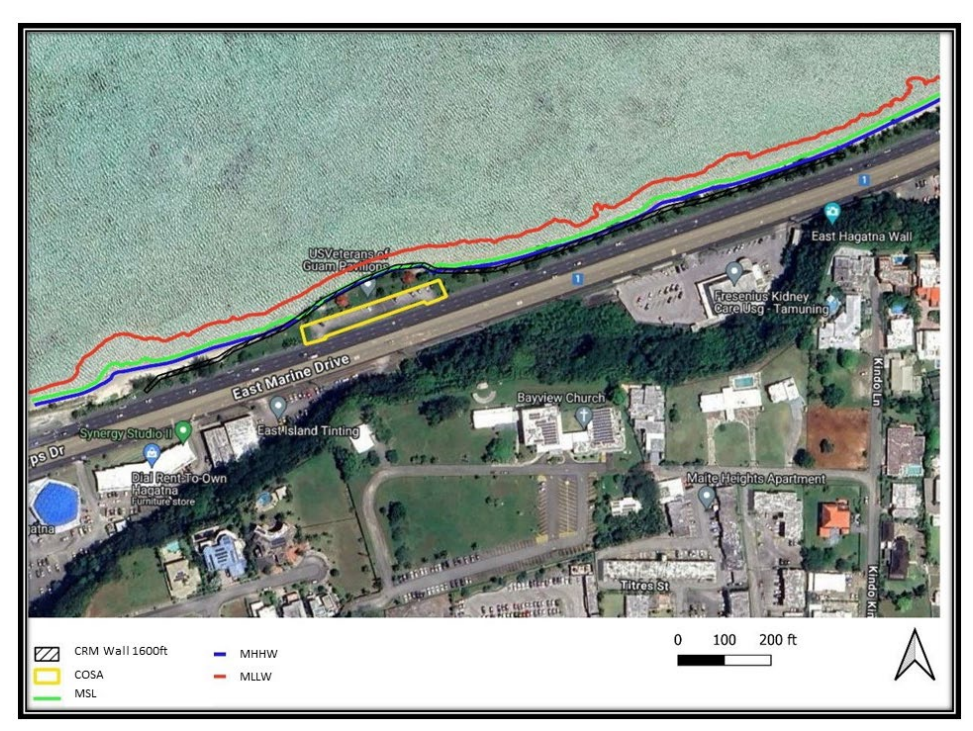


Figure 30. CRM Wall Preliminary Footprint

# Preliminary Design

The CRM wall would replace the existing sea wall and be constructed in two parts. The first, a reinforced precast concrete base, and the second, the CRM wall which would sit on top of the concrete foundation. The precast concrete base can be cast either on-site or cast off-site and transported to the site. Existing conditions indicate a natural limestone bench at -2.6 feet (MSL). The concrete base would sit on top of the limestone bench. The proposed CRM wall will act as a gravity retaining wall. Gravity retaining walls use their own weight to resist the lateral earth pressures. The typical cross section for a CRM wall is shown in Figure 31.

# HYBRID CRM WALL TYPICAL DETAIL

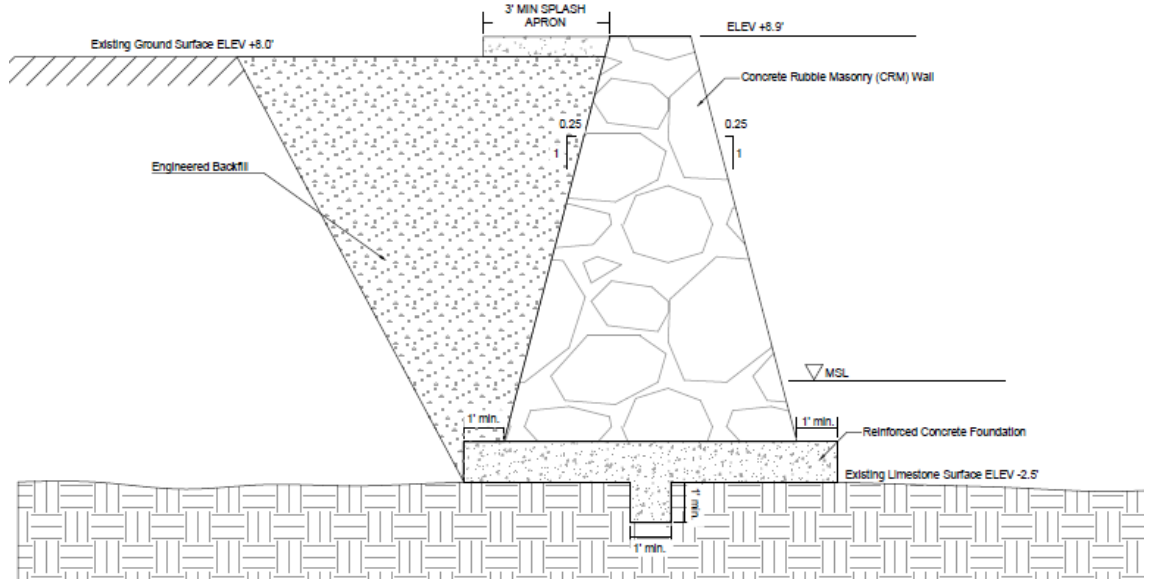


Figure 31. Preliminary CRM Wall Schematic

### Construction

Construction of the CRM wall would consist of excavating approximately two to three feet of coastal soils and placing the reinforced concrete foundation on the limestone shelf. Following the construction of the reinforced concrete foundation, a CRM wall will be installed to the planned project heights (+8.9 ft MSL). After the CRM wall is constructed on top of the concrete foundation, the area should be regraded to the elevation of the existing ground surface. Based on the proposed CRM cross-section, the final footprint would be approximately 9 feet with the total disturbed area being approximately 20 feet due to excavation and backfill of the existing soils. In addition to the approximately 20 feet of disturbed area, a minimal additional 30 feet will be needed landward of the disturbed area for the working platform of the construction equipment.

#### **Adaptation Measures**

Adaptation measures for the CRM wall, to provide adequate shoreline protection within the 100-year adaptation horizon are similar to the measures discussed for the Precast Concrete Wall. Considering the high SLC curve, under an extreme event like Typhoon Pongsona, the water levels will rise on the reef resulting in inundation of the upland as well as increased wave energy at the shoreline. Adaptation strategies to consider in the future to increase the level of protection from overtopping and submergence, would be to raise the crest height of the wall structure. Based on the amount of increase in elevation, the width of the foundation may also need to be increased in order for the structure to remain stable.

### 4.7. Secant Wall (Screened Out)

Secant piling is a robust, rigid system which can be used to construct earth retention walls. A secant wall is a vertically oriented structure, constructed shore-parallel along the shoreline, to

protect from overtopping due to waves and water levels and to fix the shoreline so erosion cannot occur landward. A secant wall is comprised of drilling overlapping concrete columns. Preliminary Design

The Secant wall could replace the existing seawall or the position could also be shifted to the landward side of the seawall. The benefit of placing the secant pile wall behind the existing wall is added flexibility to the construction schedule, and/or a cost savings on demoing the existing seawall. Secant walls overlap individual piles which allows for flexible layouts accommodating linear or curved alignments with multiple corners.

Vertical reinforcement is typically installed only in secondary piles and may be either a steel pile or rebar cage. The top elevation of the structure will be +8.9 feet MSL. The preliminary secant wall schematic is shown in Figure 32.

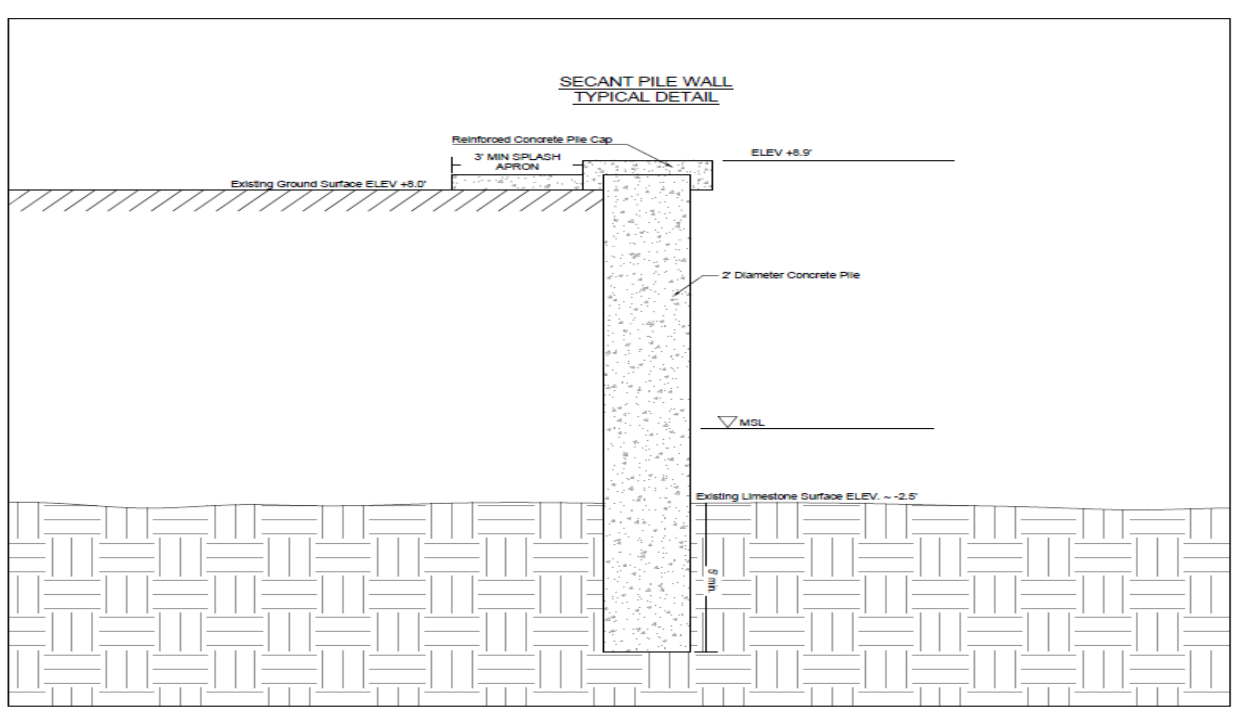


Figure 32. Preliminary Secant Wall Schematic

#### Construction

The continuous secant wall is constructed by drilling overlapped concrete. A wide range of drilling techniques can be employed allowing the secant pile walls to be constructed in variable ground conditions. The initial or "primary" piles are drilled into existing ground at the selected center spacing. The wall is completed by drilling structurally reinforced "secondary" piles which cut into and overlap with the adjacent primaries.

#### Screening

The equipment and quantity of concrete required for this measure is significant and would have to be imported from off island. Installation would require specialized drilling equipment that may not be available on island. The import of the specialized equipment and amount of concrete required for this alternative significantly increase the construction costs in comparison to the other measures.

### 4.8. Permeation Grouting (Screened Out)

Permeation grouting would not replace the existing seawall, but would act to stabilize the foundation of the wall through injection of a flowable grout into granulated soils to fill

cracks or voids and form a solid cemented mass. Permeation grouting offers the advantages of being easily performed where access and space are limited, and where no structural connection to the foundation being underpinned is required. A common application of permeation grouting is to provide both excavation support and underpinning of existing structures adjacent to an excavation. It can typically be accomplished without disrupting normal facility operations.

### Preliminary Design

Permeation grouting transforms granular soils into sandstone-like masses by filling the voids with low viscosity, non-particulate grout. Sands with low fines content are best suited for this technique. The grouted soil has increased strength, stiffness, and reduced permeability. A full analysis would need to be completed to accurately determine the recommended hole spacing. The current assumption is that a five-foot diamond grid pattern of permeation grout holes would be adequate to repair and support the existing wall. The grout holes would need to be extended a minimum of one foot into the existing limestone shelf. The preliminary permeation grouting schematic is shown in Figure 33.

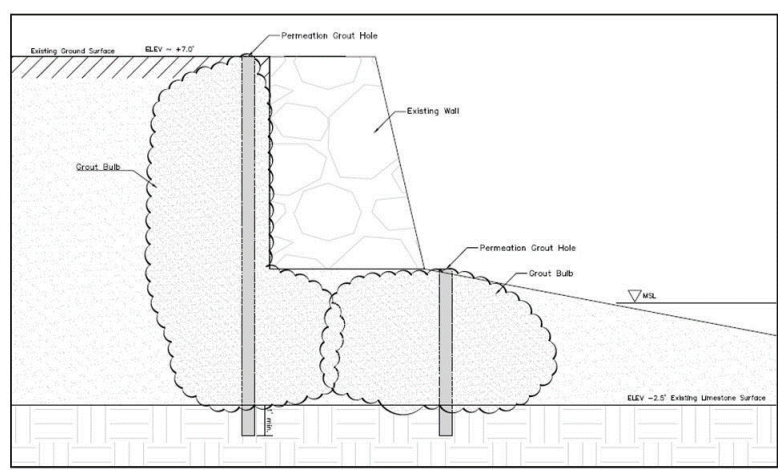


Figure 33. Preliminary Permeation Grouting Schematic

### Construction

The permeation grouting would be implemented underneath and behind the existing seawall. Permeation grouting is typically completed by first grouting a sleeve port pipe into a pre-drilled hole. The chemical grout is injected under pressure through the ports. The grout permeates the soil and hardens, creating a sandstone-like mass. The final footprint would be approximately 2 feet landward and 2 feet seaward of the existing wall. In addition, a minimal additional 30 feet will be needed landward of the disturbed area for the working platform of the construction equipment.

### Screening

Installation of this measure would require specialized equipment and materials that may not be available on island. Also, given that this measure is typically implemented to provide temporary support, this measure does not meet the standard 50-year engineering design life.

### 4.9. Beach Nourishment (Screened Out)

Beach Nourishment consists of beach quality sand added from an adjacent or outside source to nourish an eroding beach (Figure 34). Such nourishment widens the beach and extends the shoreline seaward. Beach nourishment is suitable in low-lying oceanfront areas with available sources of beach quality sand or other native sediments. Vegetated dunes help anchor sand and provide a buffer to protect inland areas from waves, flooding and erosion. Dunes can be strengthened by inclusion of a geotextile tube or rock core. Advantages include the expansion of usable beach area, lower environmental impact than hard structures, flexibility, and ease of redesign along with provision of habitat and ecosystem services. Vegetation can be planted on the dune to increase its resilience to storm events. Disadvantages however include continual sand renourishments required, limited high water protection, application is limited, and there are possible impacts to regional sediment transport. Environmental considerations include large physical footprint requirement, moderate environmental impact, impacts may be reversible, and permitting is required.



Figure 34. Beach nourishment with and without dune vegetation measure

# Screening

Considering the narrow beach profile of the study area and the observed erosion, widening of the beach footprint, through beach nourishment, could provide some additional protection to the roadway. However, as a location with a limited sediment supply, a source of beach quality sand was not identified. Additionally, the need for regular renourishments would be difficult for the non-federal sponsor to maintain, limiting the longevity of this measure.

#### 7. Summary

The engineering analysis and conceptual designs presented in this appendix were used to develop material quantities as input into the initial cost estimates and to evaluate the suitability of each alternative based on cost, environmental impact, constructability, performance, maintenance, and adaptability under future RSLC conditions. The main report and other appendices present the full analysis, which identified the Precast Concrete Wall as the Tentatively Selected Plan based on the least cost alternative that meets the study objectives.

#### 6. References

- Ahrens,. J. P. 1977. "Prediction of Irregular Wave Overtopping," CERC CETA 77-7, US Army Engineer Waterways Experiment Station, Vicksburg, MS.
- Ahrens, J. P., and McCartney B. L. 1975. "Wave Period Effect on the Stability of Riprap," Proceedings of Civil Engineering in the Oceans/III, American Society of Civil Engineers, pp. 1019-1034.
- Brunsdon, D. R. (1993). "The August 8, 1993 Guam earthquake", Bulletin of the New Zealand Society for Earthquake Engineering, 26 (4): 390–410, doi:10.5459/bnzsee.26.4.390-410
- Department of the Army. Incorporating Sea Level Change in Civil Works Programs. Engineer Regulation (ER) 1100-2-8162. June 2019.
- EQE International (1998). "Typhoon Paka December 1997" (PDF). Archived from the original (PDF) on 2012-09-05. Retrieved 2010-04-14.
- Federal Emergency Management Agency (FEMA) (2003). "Update on Recovery Efforts in Guam and Rota following Super Typhoon Pongsona". Archived from the original (DOC) on September 30, 2006. Retrieved 2007-06-29.
- Gillespie, B. (2002). "Hope Prevails Amid Complex Recovery in Guam". RedCross.org. Archived from the original on 2008-02-06. Retrieved 2007-07-23.
- Gourlay, M. R. (1996). "Wave set-up on coral reefs. 2. Set-up on reefs with various profiles," Coastal Engineering 28, 17-55.
- Lander, J. F., Whiteside, L. S., and Lockridge, P. A. (2002). A brief history of tsunamis in the Caribbean Sea. Science of Tsunami Hazards, 20(2), 57-94.
- Massey, T.C., M.E. Anderson, J.M. Smith, J. Gomez, and R. Jones. 2011a. STWAVE: Steady-state spectral wave model user's manual for STWAVE, version 6.0. ERDC/CHL SR-11-1.U.S. Army Engineering Research and Development Center, Vicksburg, MS.
- Merrifield, M. A. 2011. A shift in western tropical Pacific sea level trends during the 1990s. In Journal of Climate, Vol. 24, 4126–4138, doi:10.1175/2011JCLI3932.1.
- Merrifield, M. A., P. R. Thompson, and M. Lander. 2012. Multidecadal sea level anomalies and trends in the western tropical Pacific. In Geophysical Research Letters, Vol. 39, L13602, doi:10.1029/2012GL052032.Widlansky 2015
- Merrifield, M. and M. Maltrud. 2011. Regional sea level trends due to a Pacific trade wind intensification. In Geophysical Research Letters, Vol. 38, L21605.
- National Climatic Data Center (NCDC) (1997). "Event Report for Typhoon Paka". Archived from the original on 2010-12-24. Retrieved 2010-04-14.
- National Center for Environmental Information (NCEI) (2002). "Storm Data and Unusual Weather Phenomena with Late Reports". 44(12). National Oceanic and Atmospheric Administration: 119-121. Retrieved from: https://www.ncei.noaa.gov/pub/orders/IPS/IPS-23A58EBE-8D3F-4014-AD12-834FADBDB8A7.pdf
- Rupp, J. A., and Lander, M. A. (1996). A technique for estimating recurrence intervals of tropical cyclone-related high winds in the tropics: Results for Guam. Journal of Applied Meteorology and Climatology, 35(5), 627-637.
- Seelig, W. N. (1983). "Laboratory study of reef-lagoon system hydraulics," Journal of Waterway, Port, Coastal and Ocean Engineering 109(4), 380-391.
- Smith, J. M., A. R. Sherlock, and D. T. Resio. 2001. STWAVE: Steady-state spectral wave model, user's guide for STWAVE version 3.0, ERDC/CHL SR-01-01, U.S. Army Engineer Research and Development Center, Vicksburg, MS, 80 pp.
- Smith, J. M., & Smith, S. J. 2002. Grid nesting with STWAVE (No. ERDC/CHL CHETN- 1-66). Engineering Research and Development Center, Vicksburg, MS. Coastal and Hydraulics Lab.
- Weir, R.C. (1983). Tropical cyclones affecting Guam (1671-1980). Naval Oceanography

# 7. Model Output Appendix

As water level increases in the area, larger waves are able to propagate nearshore. The greatest wave heights per water level scenario were observed for the top ranked event and the 100-year wave event out of the north, 351 and 0 degrees, respectively. The lowest wave heights per water level scenario were observed for the 10-year wave event from the 270-degree direction (westerly).

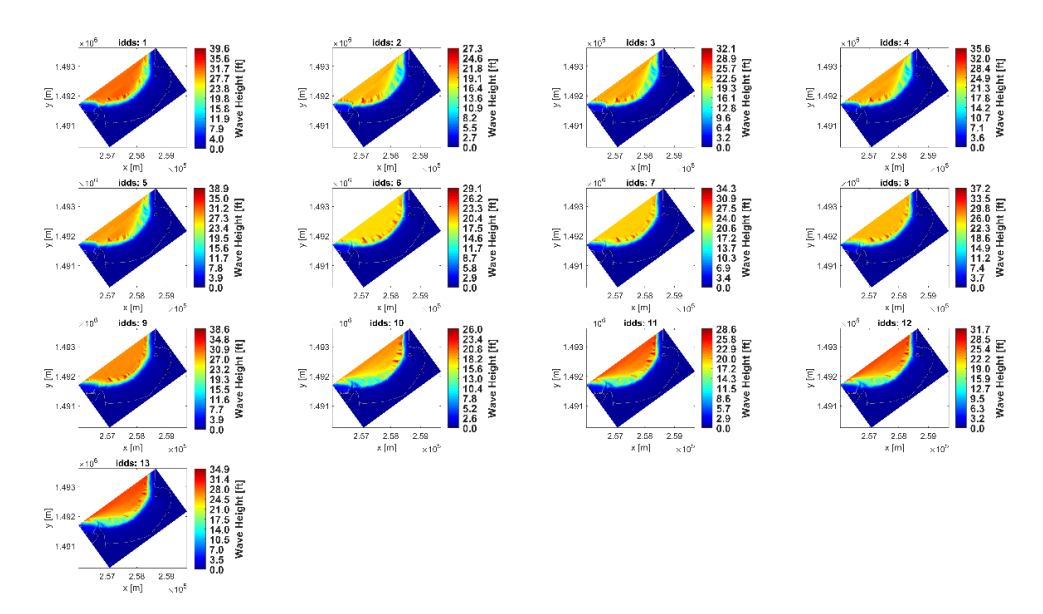


Figure 35. MSL

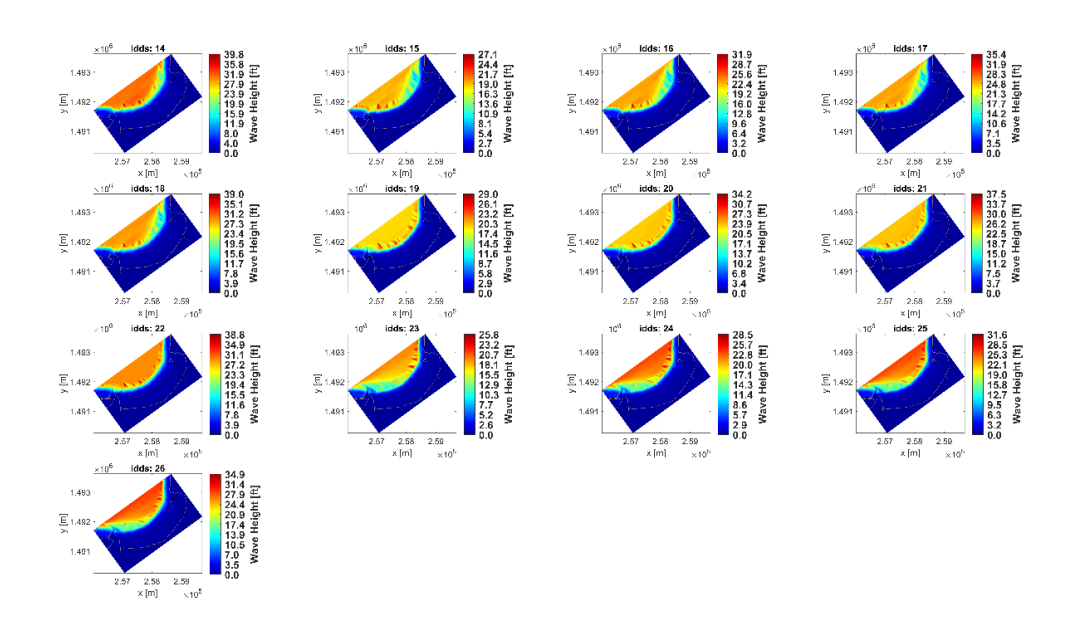


Figure 36. MHHW

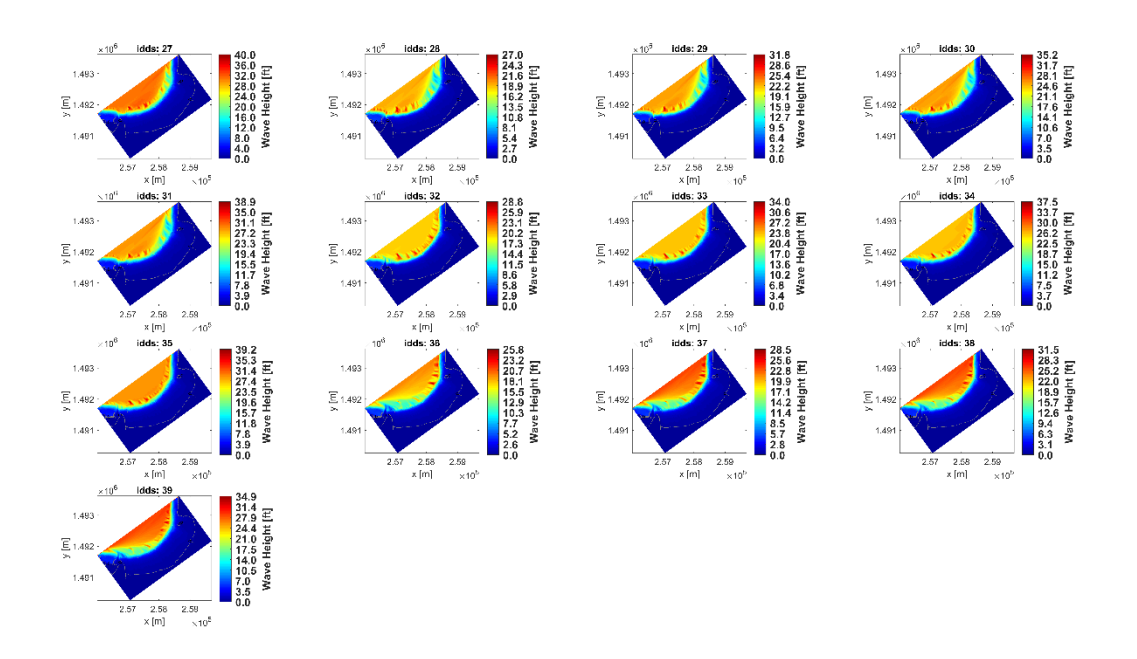


Figure 37. MHHW+2%AEP

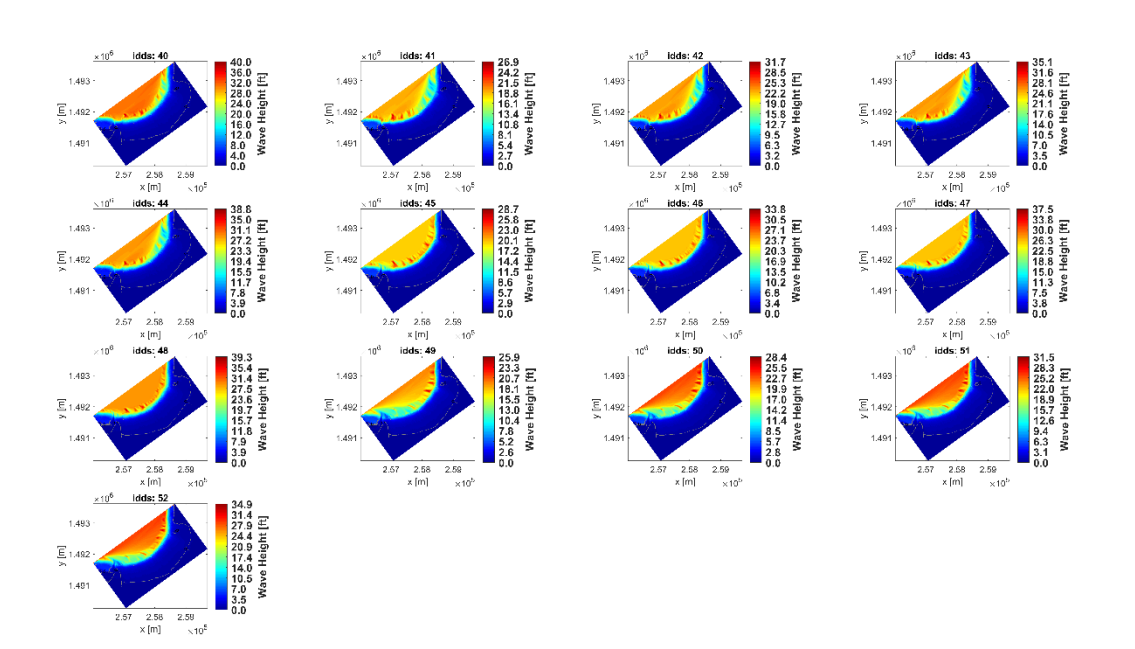


Figure 38. MHHW+2%AEP+25LowSLC

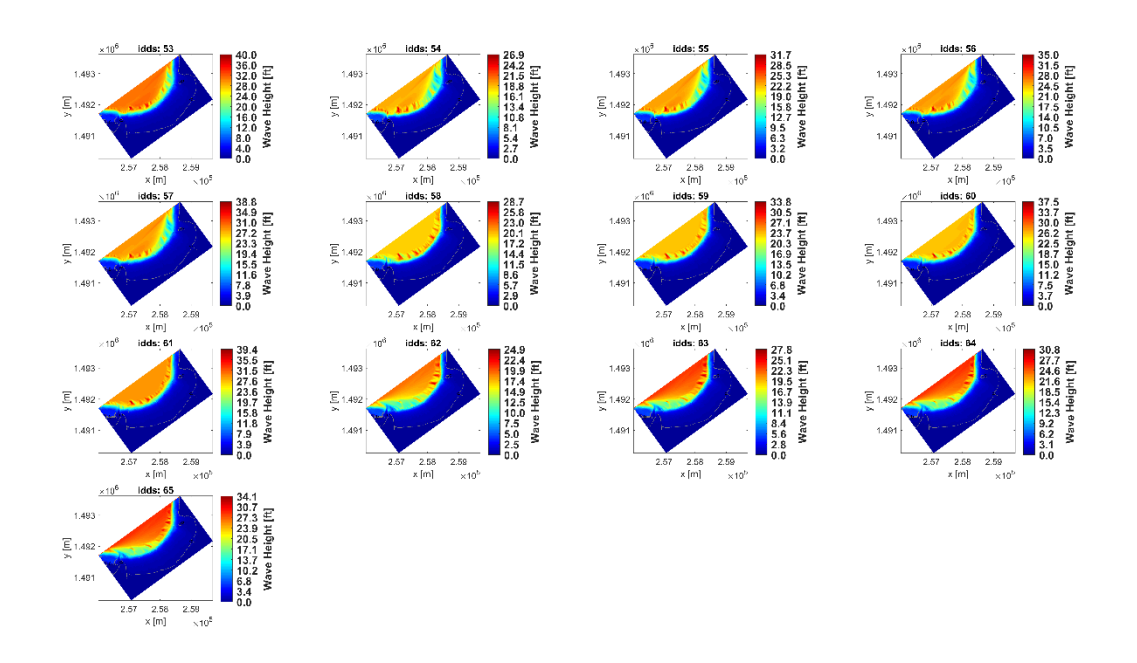


Figure 39. MHHW+2%AEP+50LowSLC

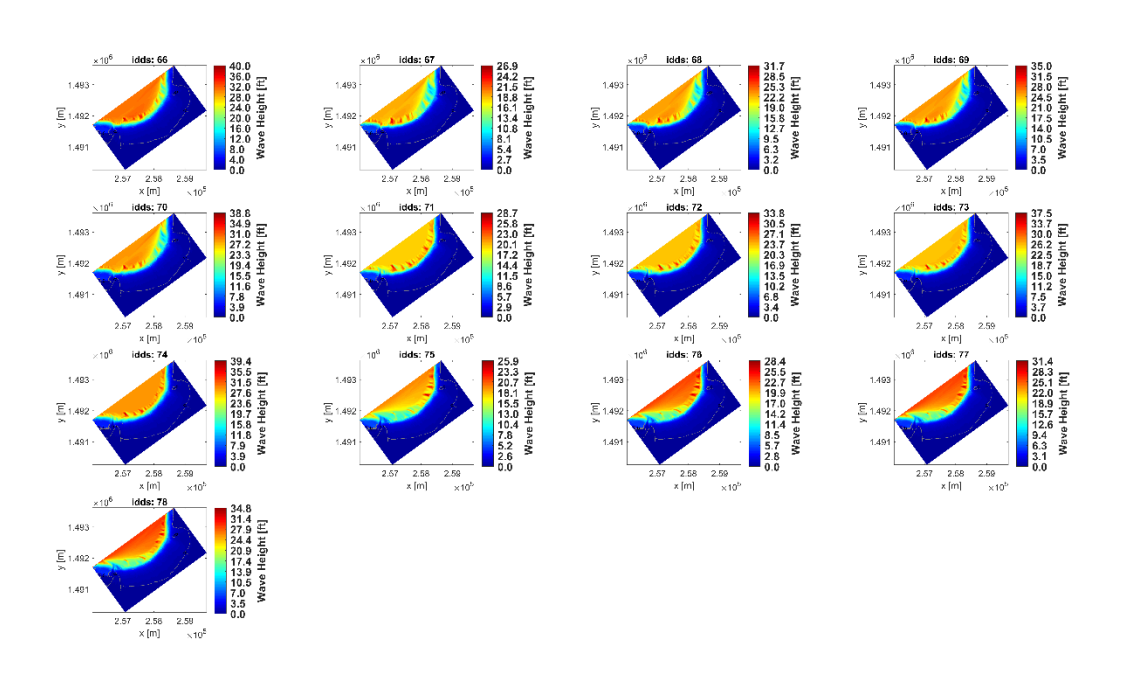


Figure 40. MHHW+2%AEP+25IntermidateSLC

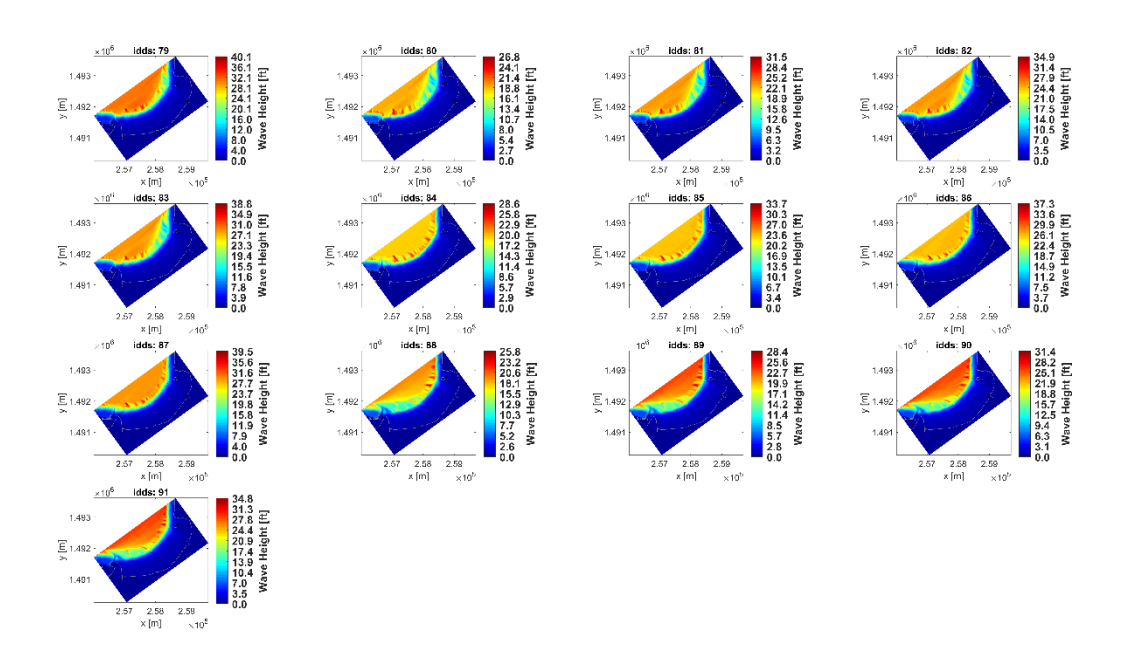


Figure 41. MHHW+2%AEP+50IntermediateSLC

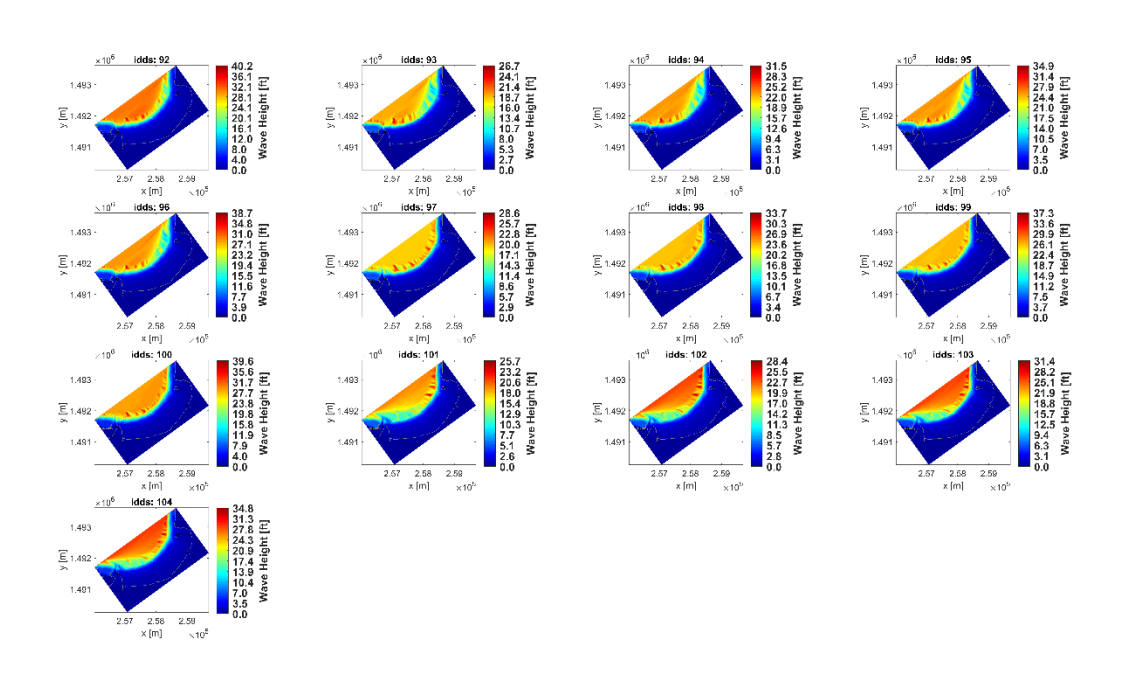


Figure 42. MHHW+2%AEP+25HighSLC

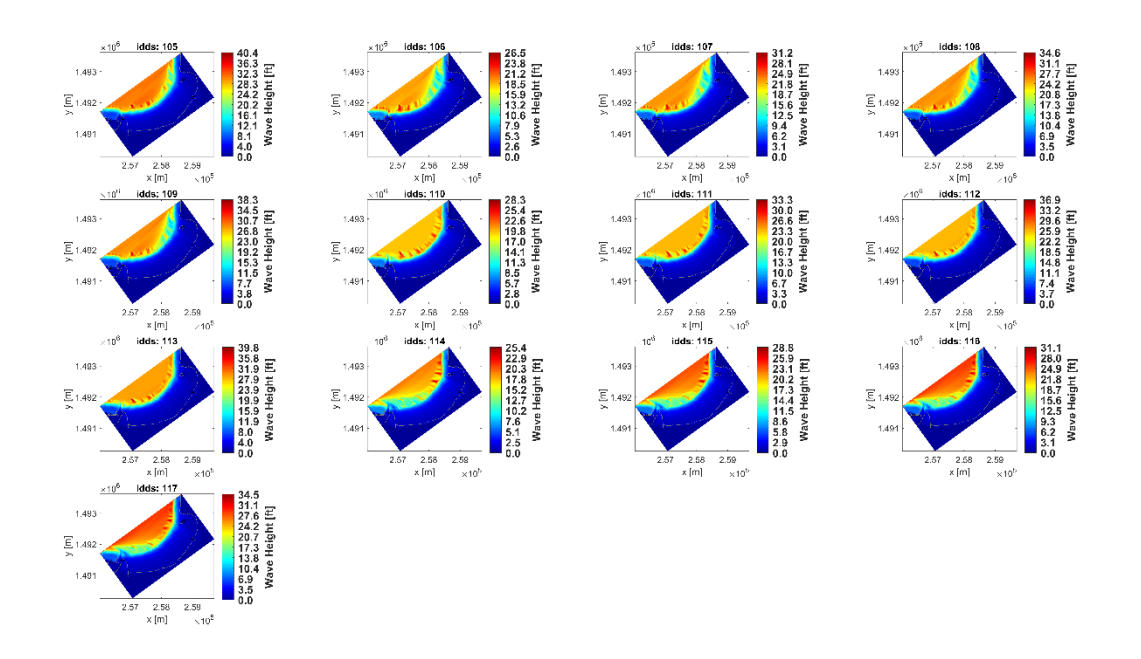


Figure 43. MHHW+2%AEP+50HighSLC

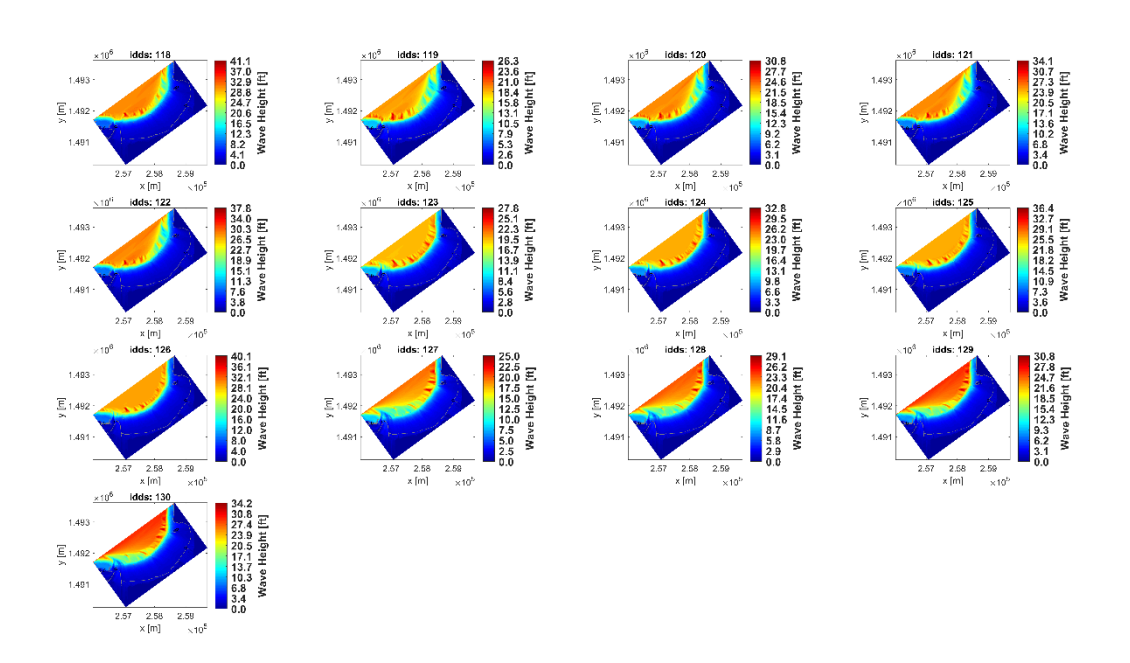


Figure 44. MHHW+2%AEP+100LowSLC

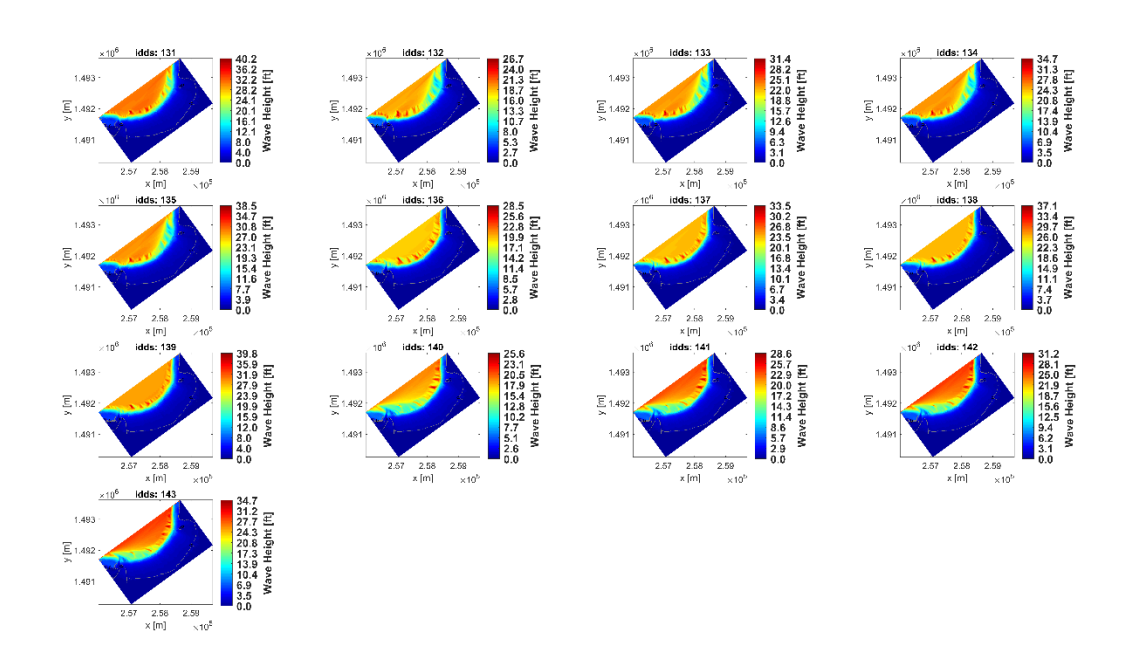


Figure 45. MHHW+2%AEP+100IntermeidateSLC

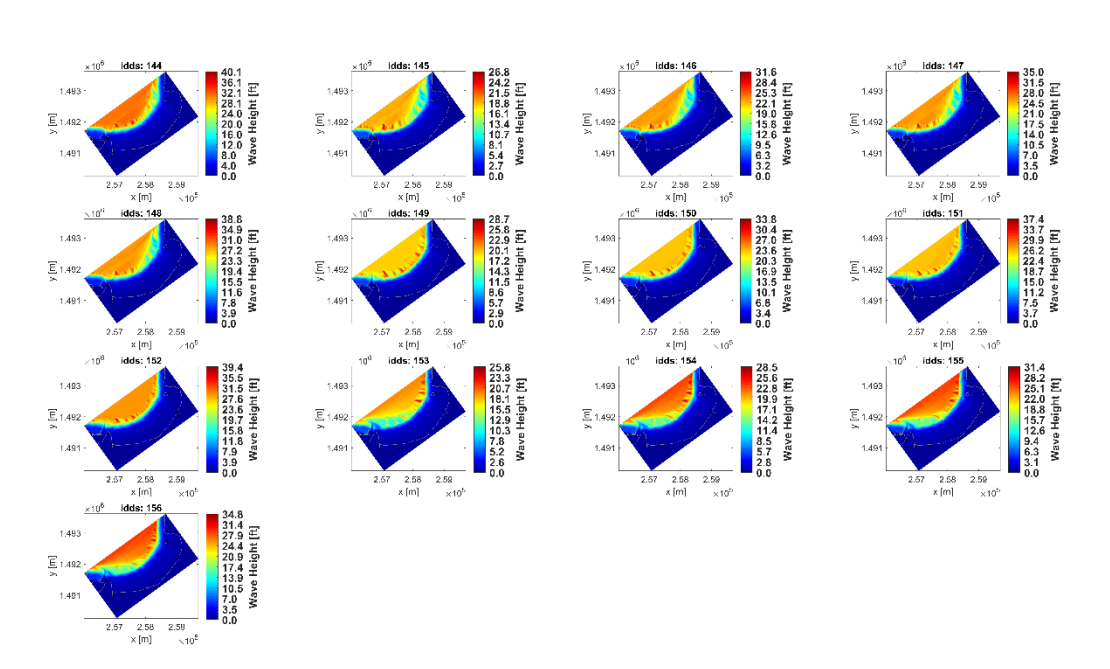


Figure 46. MHHW+2%AEP+100HighSLC